Texas A&M University

Department of OCEANOGRAPHY

AN INVESTIGATION OF CHANGES INDUCED IN MACROSTRUCTURES IN PELITIC SEDIMENTS DURING PRIMARY CONSOLIDATION

TECHNICAL REPORT
Reference 70-8-T

TAMU-SG-70-215
ONR contract N00014-68-A-0308(0002)
USGS contract 14-08-0001-11990

Research conducted through the Texas A&M Research Foundation and Sea Grant Programs Office.
College Station, Texas

TEXAS A&M UNIVERSITY

College Station, Texas

Research conducted through
the Texas A&M Research Foundation
and Texas A&M Sea Grant Office

Projects 53570, 53571,
700-8, 700-9,
and 663

AN INVESTIGATION OF CHANGES INDUCED IN MACROSTRUCTURES IN PELITIC SEDIMENTS DURING PRIMARY CONSOLIDATION

This report was partially supported by the National Science Foundation Sea Grant Program institutional Grant GH59 made to Texas A&M University under Texas A&M University Account #53570 and 53571;
The Office of Naval Research, contract N00014-68-A-0308-(0002) under Texas A&M Research Foundation projects 700-8 and 700-9;
and Department of the Interior, U.S. Geological Survey, contract 14-08-0001-11990 under Texas A&M Research Foundation project 663.

Report prepared January 1970

by

Frank Bernard Chmelik

FORWARD

The following report is based on a dissertation submitted by Mr. Frank B. Chmelik in partial fulfillment of the requirements for a Doctor of Philosophy degree in Oceanography at Texas A&M University.

One of the problems in dealing with recent and ancient deposits is the correlation of sedimentary characteristics in order to use one as a key to the other for interpretation purposes. The influence of consolidation upon sediments and sedimentary structures results in various changes which can be of both physical and chemical origin.

The Geological Oceanography Section is involved in a study on changes of sedimentary properties under the influence of consolidation making use of cores collected from the Gulf of Mexico and consolidometers used for geotechnical investigations.

This report presents the first phase of this study. Artificial as well as natural shaped structures were subjected to consolidation and their changes analyzed.

Deep water samples used in this study were collected under a grant provided by the Office of Naval Research under contract N00014-68-A-0308 (0002), Research Foundation Projects 700-8 and 700-9.

Information from shallow water cores was obtained with the help of a research project funded by the United States Geological Survey, Contract 14-08-0001-11990, Research Foundation Project 663.

The electrical logging technology used in support of this study was partially supported by the National Science Foundation Sea Grant Program institutional Grant GH59 made to Texas A&M University under

Texas A&M University Accounts #53570 and 53571. Mr. Chmelik was activity leader of this Sea Grant project.

Arnold H. Bouma
Project Supervisor
Projects 663 and 700-9

William R. Bryant
Project Supervisor
Project 700-8

ABSTRACT

This investigation of consolidation-induced changes in macrostructures is based on (1) the use of stereo X-ray radiography to map the macrostructures prior to and following consolidation and (2) a comparison of changes induced in artificial and natural macrostructures. Homogeneous marine clay, fine grained quartz sand, and CuO powder were used to make twenty-two geometric macrostructures.

Several types of coring devices, including two Flexible Liner Corers developed for this study, were used to collect cores from a variety of depositional environments.

Electrical logging techniques and X-ray radiography were applied to locate and identify macrostructures in the cores. The cores were cut longitudinally to allow photography, half-core X-ray radiography, and visual inspection of the structures. Selected macrostructures were removed from the core halves, rejoined, placed into PVC consolidometer cylinder liners and consolidated.

Stereo X-ray radiographs were made in at least two orientations, both immediately prior to and following consolidation of all models. Primary consolidation for a load of 32 TSF was effected on the macrostructures in Anteus Back Pressure Consolidometers.

Comparisons of the macrostructure changes induced during consolidation of the artificial structures with those of the natural structures indicates the existence of a positive relationship. Several conditions are imposed before the natural and artificial structures can be related. These conditions include that both structures be of

similar materials and subjected to similar conditions of consolidation. This relationship may allow the analysis of consolidated natural macrostructures by comparison with consolidated artificial models and possibly lead to a method of relating the natural macrostructures to their environment of deposition.

ACKNOWLEDGEMENTS

The writer wishes to thank members of his committee, Drs. A.H. Bouma, W.R. Bryant, D.A. Fahlquist, R. Rezak and Mr. F.E. Smith for their useful suggestions during the research and editing phase of this study. Thanks is also given to Drs. Edward Ibert and Park Snavely, former committee members, for their help during the planning stage of this study.

Acknowledgement is also made of the use of samples collected in connection with the contractions mentioned in the Forward of this report.

Sea Grant projects 53570 and 53571 supported the electrical logging development program. The writer wishes to express his gratitude to the Sea Grant Office for funding this program as well as for the experience gained while activity leader of the project.

A special thanks is given to Mr. Robert Mayer, Jr. and Mr. Ray McConnel of Well Reconnaissance, Inc., of Dallas, Texas. Without their active participation in the Sea Grant Program on electrical logging, this study would have been lacking a major technique.

TABLE OF CONTENTS

TABLE OF CONTENTS, CONT. Page

LIST OF TABLES

Table Page

LIST OF FIGURES

LIST OF FIGURES - APPENDICES

INTRODUCTION

The purpose of this research is to investigate the changes which occur in macrostructures of pelitic sediments during primary consolidation. For use in this study the terms "macrostructure" and "primary consolidation" are defined.

Macrostructures are morphological features formed by the spatial relationship between two or more adjacent materials, are small enough to be manageable in the laboratory, and large enough to be discerned by the unassisted eye. These structures are commonly associated with recently deposited sediments and in some cases appear to be related to specific environments of deposition.

A sediment is said to be undergoing primary consolidation during the time the free interstitial water is being forced from the void spaces in response to an applied load. For any one load, the end point of primary consolidation occurs when the excess pore water pressure is zero.

The specific objectives are:

(1) to investigate the behavior of artificial, geometric models of pelitic sedimentary macrostructures during primary consolidation,

(2) to investigate the behavior of natural pelitic sedimentary macrostructures during primary consolidation, and

---

The citations on the following pages follow the style of Marine Geology.

(3) to relate the changes noted in (1) and (2) above and examine the possibility that consolidation-induced changes in natural macrostructures may be analyzed by comparison with segments of one or more consolidated geometric models. (i.e., by matching the parts of a consolidated macrostructure with similarly shaped segments of consolidated geometric models, we may be able to describe by inference the macrostructure prior to consolidation.)

This research will add to our knowledge of the mechanics of deformation of sedimentary macrostructures and may suggest methods that may be useful in relating structures in consolidated pelitic materials to their environment of deposition (RAINWATER, 1966). In addition, the techniques and methods developed during the course of this work will improve our ability to handle and study fragile sedimentary materials (STANLEY, 1966).

Previous work

The process of consolidation of sediments has been the subject of research by civil engineers and geologists for many years. Indeed, the field of soil mechanics, including studies of sediment consolidation, has developed as a civil engineering professional speciality (WU, 1967). TERZAGHI (1955) did much to establish the basis for modern soil mechanics and related engineering properties of sediments to the geologic characteristic of the material. KRUMBINE and SLOSS

(1963) and PETTIJOHN (1949) gave considerable attention to macrostructures in consolidated lithified sediments.

The work of CAYEUX (1941) was a significant contribution in relating macrostructures in lithified sediments to their environment of deposition. Because of the economic importance of this relationship and its usefulness in the interpretation of geologic history the problem was approached by many other investigators (JACKA, THOMAS, BECK, WILLIAMS and HARRIS, 1967; CHUBER and PUSEY, 1967; COOGAR, 1967; HORWITZ, 1967; GREENSMITH, 1967; etc.). Studies relating lithified macrostructures to their environments of deposition have been almost exclusively concerned with structures in sediments of predominently sand-size grains (ripple marks, cross-bedding, etc.).

It has been only in comparatively recent times that macrostructures in unconsolidated sediments have been extensively studied in relation to their environments of deposition (VAN STRAATEN, 1959; SHEPARD, 1964; BRIGGS and MIDDELTON, 1965; BRUSH, 1965; etc.).

The consolidation and lithification of some types of recent marine sediments has been discussed by HAMILTON (1959). Other investigators who have contributed in this area include MOORE and SCRUTON (1957), SANDERS (1965) and MONROE (1969).

COLEMAN and GAGLIANO (1965) and KOLB and VAN LIPIK (1966) describe in detail a number of macrostructures in the pelitic sediments of the Mississippi River deltaic plain, and identify their environments of deposition. KRINITZSKY and SMITH (1969) subdivided and correlated the backswamp deposits underlying most of the

Atchafalaya Louisiana levee system based on X-ray radiography. They included observations of fracturing and plastic deformation of the soils and noted the presence of organic matter, secondary mineralization, burrows, and other features. However, changes induced in pelitic sedimentary macrostructures during primary consolidation have received little or no direct attention by researchers. There are several possible reasons for this.

(1) Macrostructures in sand-size sediments are apparently little effected by consolidation. Therefore, when they appear in the lithologic record, the relationship to their environments of deposition is easily recognized.

(2) Recent pelitic sediments are difficult to work with because of their lack of rigidity, high water content, adhesion, cohesion, and low permeability. In addition, macrostructures associated with these sediments most often occur within the material and normally have no surface expression.

(3) Adequate techniques and methodology have not been available for laboratory studies.

EXPERIMENTAL PROCEDURE

This study compares pelitic sedimentary macrostructures (both natural and artificial) before and after primary consolidation. Two techniques are required: (1) a means of consolidating the samples, and (2) a means of making a detailed description of the macrostructures prior to and following consolidation. The first requirement was satisfied by the use of six consolidometers in the Department of Oceanography. These machines are capable of exerting an unidirectional load of 32 TSF while allowing fluid drainage along the axis of applied stress. The second requirement was met by the use of stereo X-ray radiography (APPENDIX I). The Pickert Industrial X-ray unit at the Department of Oceanography was used for this work.

In order to conduct this program, it was desirable to develop several additional techniques.

(1) A technique was needed that would allow the cutting and shaping of pelitic sediments without disturbing the macrostructures. To do this, an electro-osmotic knife was developed (APPENDIX II).

(2) Coring equipment specifically designed to preserve the fragile macrostructures in recent pelitic sediments was needed. Two Flexible Liner corers were developed (deep water and shallow water) with this capability (APPENDIX III).

(3) A non-destructive technique for the rapid location of macrostructures in cores was needed. The application of electrical logging methods provided this technique (APPENDIX IV).

(4) It was felt that a non-destructive method of mapping macrostructures other than by X-ray radiography would yield additional information. The use of color thermography was investigated for this purpose (APPENDIX V).

<u>Model study</u>

Artificial and natural models of sedimentary macrostructures were examined. A total of forty-three models were studied. Sixteen (eight natural and eight artificial) were employed in an attempt to use color thermography as a means of mapping macrostructures (APPENDIX V). The results of these experiments lead to the conclusion that, while theoretically possible, color thermography was not a practical tool for this particular study. Consequently, that avenue of investigation was abandoned.

In all, thirty-five models (twenty-two artificial and thirteen natural) were investigated before and after consolidation by means of stereo X-ray radiography (APPENDIX I). Stereo pairs were made of at least two orientations of the models prior to consolidation and again following consolidation. A minimum of three orientations were used with the natural models.

The general procedure used in preparing the models for consolidation (Fig. 1) follows.

(1) The models were cut into 2½ inch diameter cylinders. This was done with the aid of an electro-osmotic cutting ring.

Fig. 1. General procedure used in preparing the models for consolidation.

1. Sample with electro-osmotic cutting ring in place.
2. Model cut and excess material removed from sides of ring.
3. Excess material trimmed from ends of ring.
4. Cutting ring with model in position on PVC liner. Bottom porous stone is already in the liner; the top porous stone in position to extrude the model.
5. Model extruded from cutting ring into PVC liner.
6. PVC liner with model packaged in sheet plastic.
7. Pre-consolidation X-ray radiography. Model and liner in sand ballast (see APPENDIX I).

8., 9. Consolidation.

10. Model and liner removed from steel consolidation cylinder.
11. Post-consolidation X-ray radiography.
12. Consolidated model and porous stones removed from PVC liner.

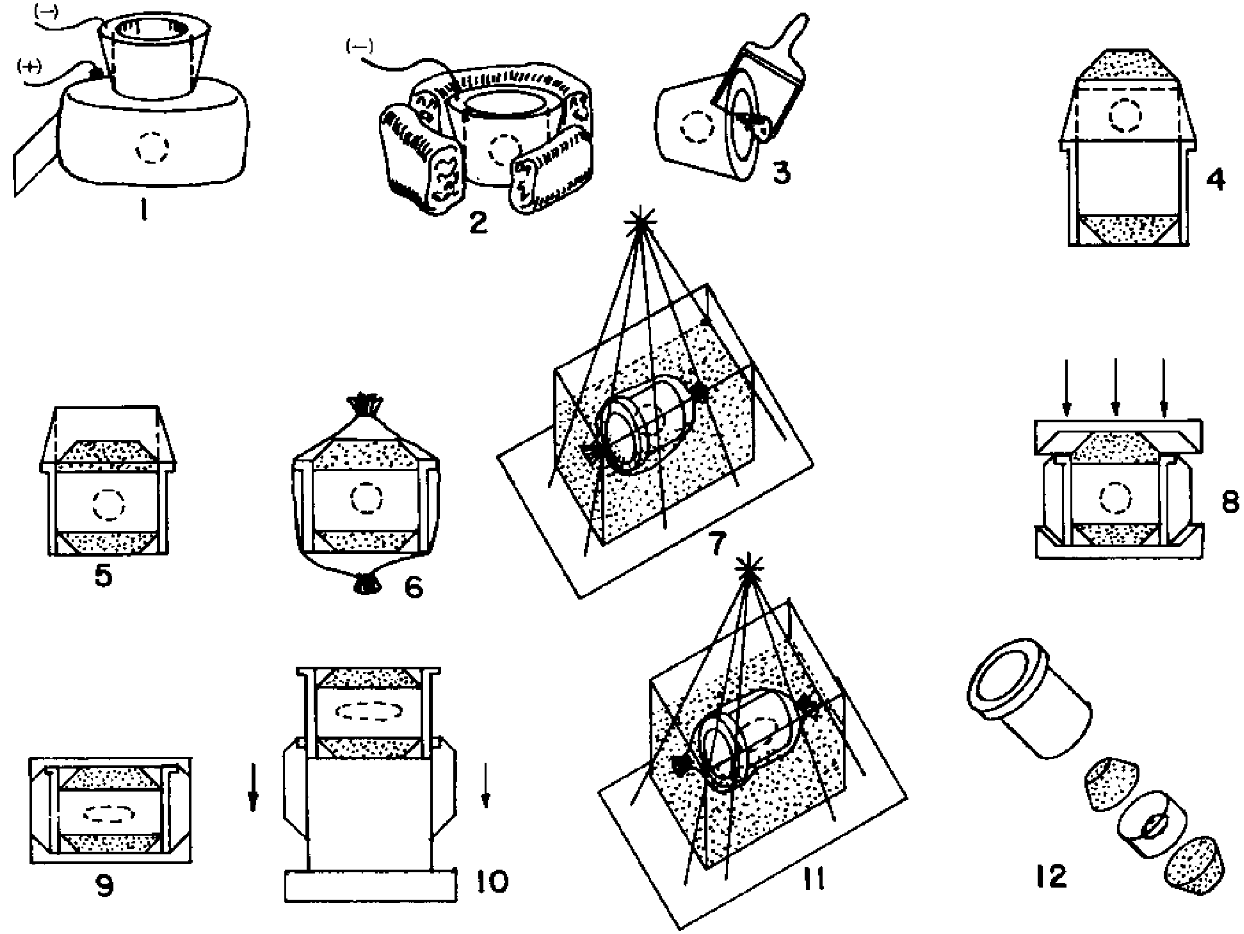
(–)
(+)
1
(–)
2
3
4
5
6
7
8
9
10
11
12

(2) The models were extruded from the cutting ring into thin-walled Poly Vinyl Chloride (X-ray transparent) consolidometer cylinder liners. To accomplish this, the model-filled cutting ring was placed on top of the liner and a porous stone used as an extrusion plunger to push the model into the liner.

(3) The models and PVC liner were labeled and then wrapped in thin-film plastic.

(4) The packaged models were placed horizontally in cardboard boxes which had X-ray transparent plastic bottoms. Fine-grained quartz sand was used to fill the boxes to the level of the top of the liners. This sand functioned as radiation ballasting to prevent uneven exposures due to the cylindrical shape of the models.

(5) Stereo X-ray radiographs were made of each model in at least two orientations. The standard orientations are A @ 0^o, B @ 90^o (measured around the cylinder) with C @ 45^o and D @ 15^o used on selected models (APPENDIX I, Fig. AI-1). Position A is established parallel to a plane of symmetry in the artificial models and chosen arbitrarily in the natural models.

(6) The model-ladened PVC liners were inserted into steel consolidation cylinders. Anteus Back Pressure Consolidometers were used to consolidate the models. The models were subjected to a load of 32 TSF until primary consolidation had been established. Excellent descriptions of this apparatus and the test procedures can be found in LOWE, et al. (1964), BUCHANAN (1967), BRYANT, et al. (1967) and

CERNOCK (1967).

(7) After consolidation, the PVC liners were removed from the steel cylinders and again packaged in plastic. Stereo X-ray radiography was repeated with the same orientations used in the preconsolidation series.

(8) The models were extruded from the liners, packaged, labeled, and stored under refrigeration.

Artificial models

A series of twenty-two artificial macrostructures with simple, three-dimensional, geometric figures (forms inside of the model) was constructed in order to investigate consolidation-induced changes in basic shapes (Fig. 2). Primary material for these models was marine clay taken from the "flow-in" of a number of deep-water cores (Sigsbee Abyssal Plain).

Twenty-five pounds of this clay were blended for 24 hours in a five gallon food mixer. Filtered Gulf of Mexico sea water was added initially to bring the water content of the material up to a level consistent with easy handling. (Empirically, this was when a 1 in. diameter column of the material 3 in. high could just stand without slumping under its own weight.) After blending, the container for the clay was kept sealed to prevent evaporative losses. Samples of the clay supply were taken periodically to check water content (TABLE I).

The geometric figures were fabricated from the following combinations.

(1) Primary clay material with 50% (by weight) fine-grained quartz sand added.

(2) Primary clay material mixed with 10% (by weight) CuO powder (X-ray opaque) added.

(3) Combination of (1) and (2) above. (50% sand with 1% CuO was used to enhance the X-ray density contrast on some models.)

Fig. 2. The geometric figures planned for use as artificial macrostructure models. The diagrams on the left represent cross sections of models prepared for consolidation. Sketches on the right depict entire figures. Models 1 through 17 consist of clay with clay-quartz sand figures. Models 19 and 20 are clay figures with a thin coating of CuO powder. Models 21 and 22 are clay figures with CuO powder mixed with the clay. The stipplings represent the clay-sand mixture.

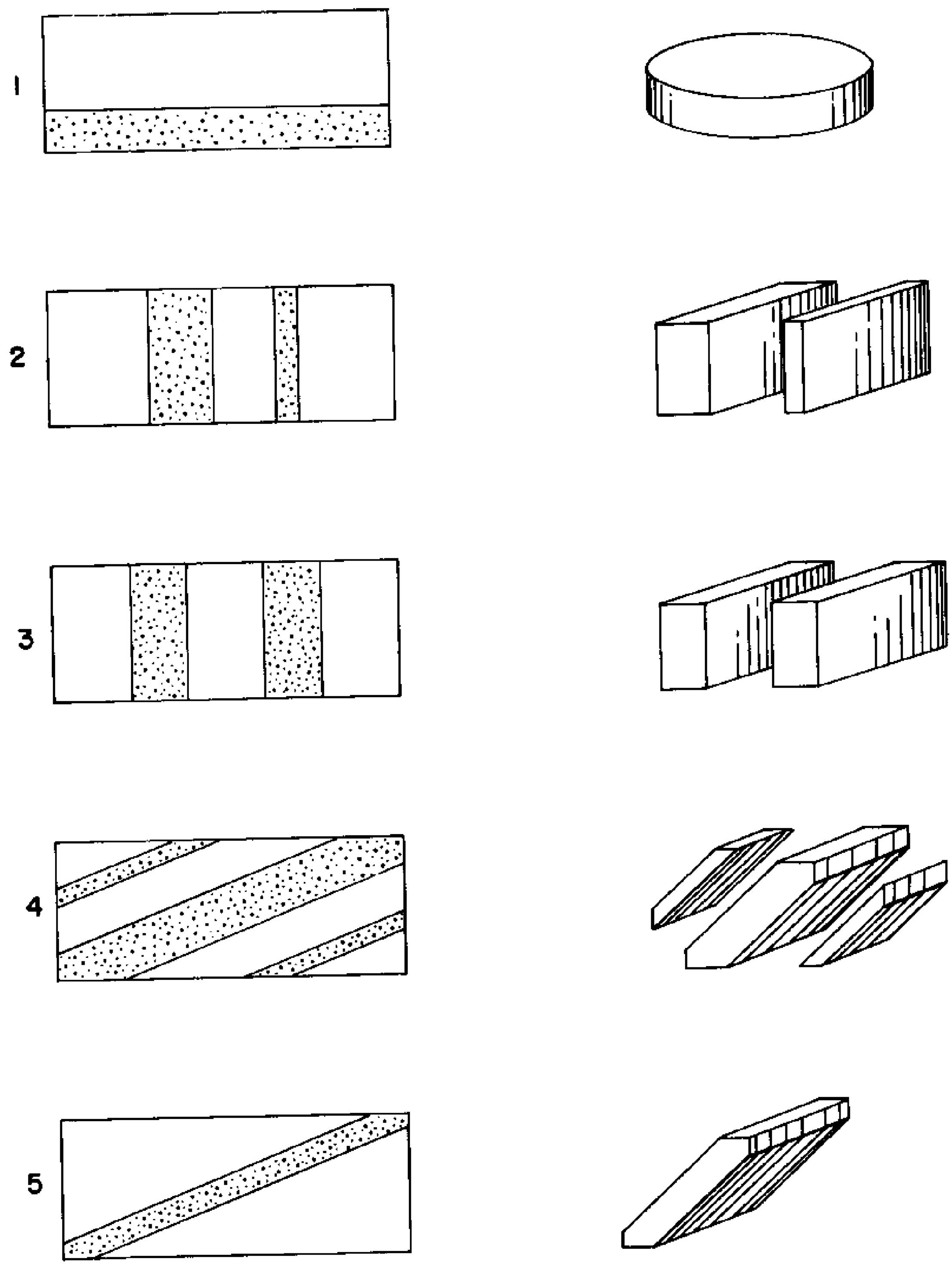
1
2
3
4
5

6

7

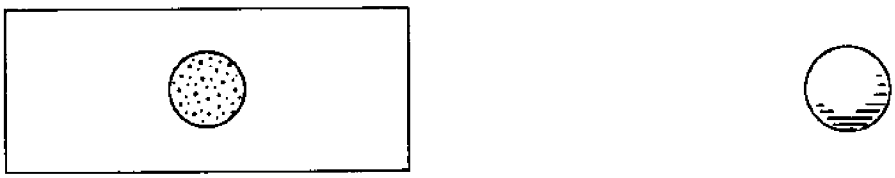

8

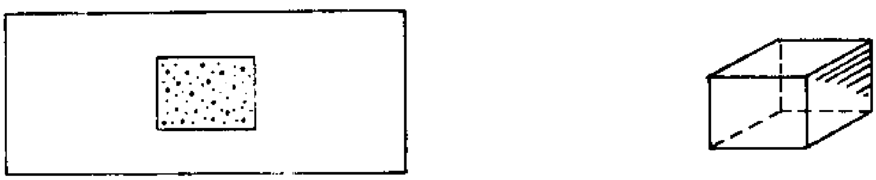

9

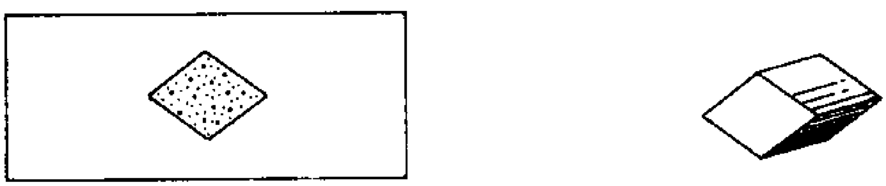

10

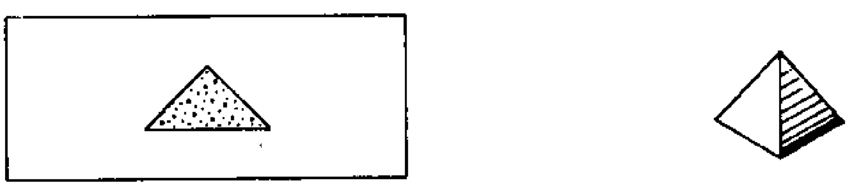

11

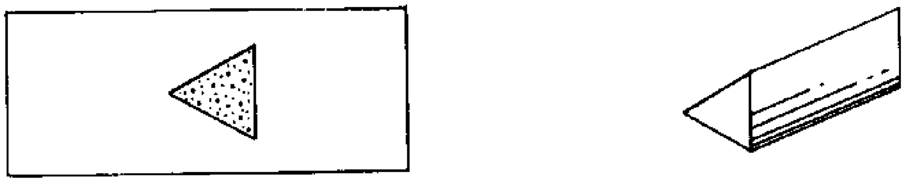

12

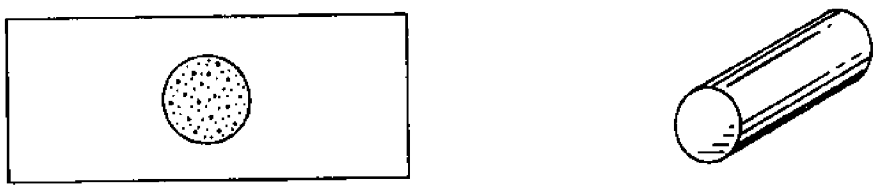

13

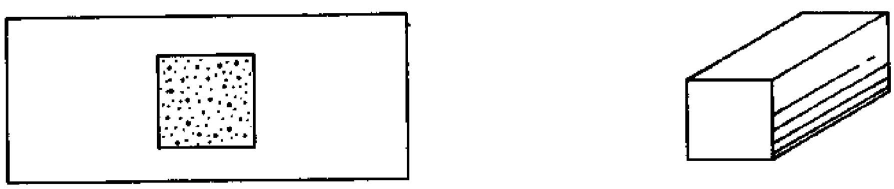

14

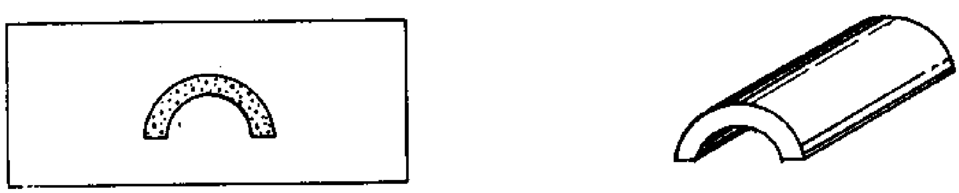

15

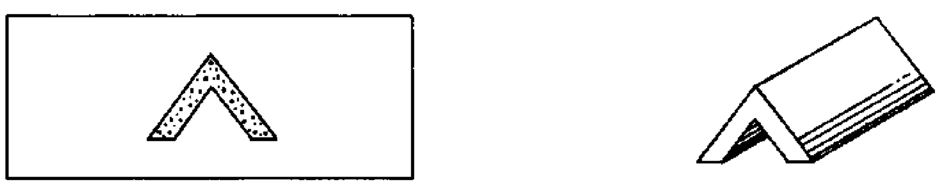

16
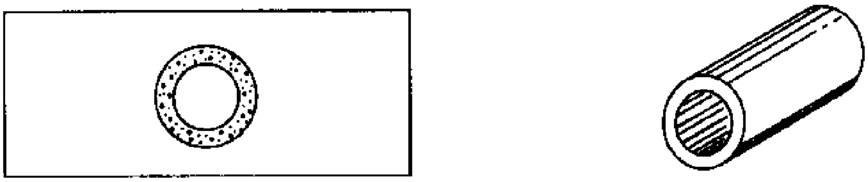

17


18
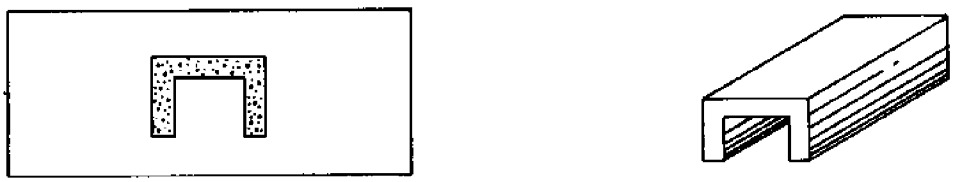

19
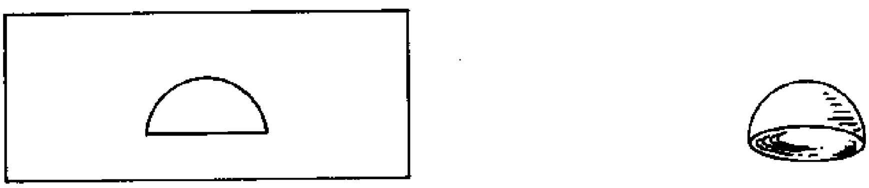

20
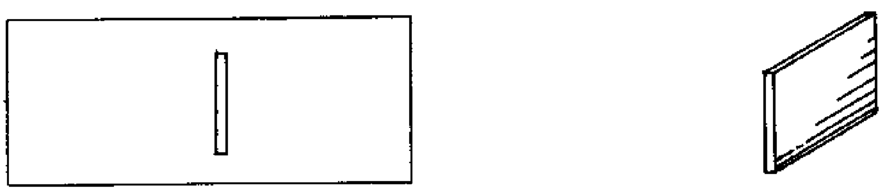

21

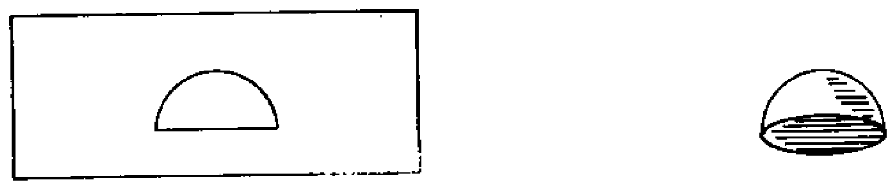

22

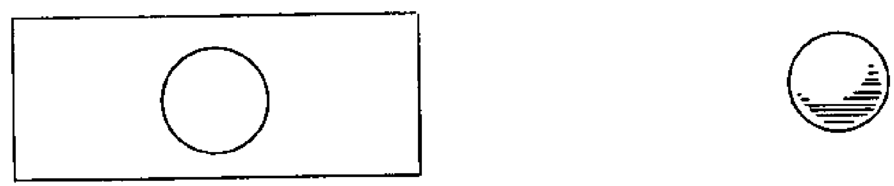

(4) Primary clay material with a surface coating of CuO powder.

Size analyses were conducted on the primary clay material (after blending) and the clay-sand mixture used for constructing figures (TABLE I). Analyses were also carried out on the quartz sand and the CuO powder (Fig. 3).

The construction procedure for the artificial models was as follows (Fig. 4).

(1) Sufficient clay material for several models was removed from the supply container.

(2) The clay was worked into a 4 in. diameter disk 2 in. thick.

(3) The materials to be used in the geometric figure were blended.

(4) The figure was created with the help of the electro-osmotic knife.

(5) The clay disk was dissected and the necessary material removed to allow the implanting of the figure.

(6) The geometric figure was implanted and the disk restored to its original shape. Slight pressure applied to the disk surfaces with the hands was usually enough to seal the disk after the parts were carefully reassembled.

(7) The model was isolated from the rest of the disk by using the electro-osmotic cutting ring. Surplus clay was removed from the ring's sides and the ends trimmed flush with the face of the ring. The result was a trimmed and oriented 2½ in. diameter model, 7/8 in. thick.

TABLE I

SAMPLE ANALYSIS

HOMOGENEOUS SEDIMENTS

TYPE	% WATER +	% SAND	% SILT	% CLAY	MD ϕ
CLAY	38.67 *	2.54	75.27	22.19	4.0
SAND - CLAY	29.03	50.31	38.34	11.35	9.64

* AVERAGE OF FOUR SAMPLES, (RANGE 37.92% TO 39.98%)

+ ALL PERCENTAGES ARE BY WEIGHT

Fig. 3. Analysis of quartz sand and CuO powder used in artificial models.

SIZE ANALYSIS

QUARTZ SAND AND CuO POWDER

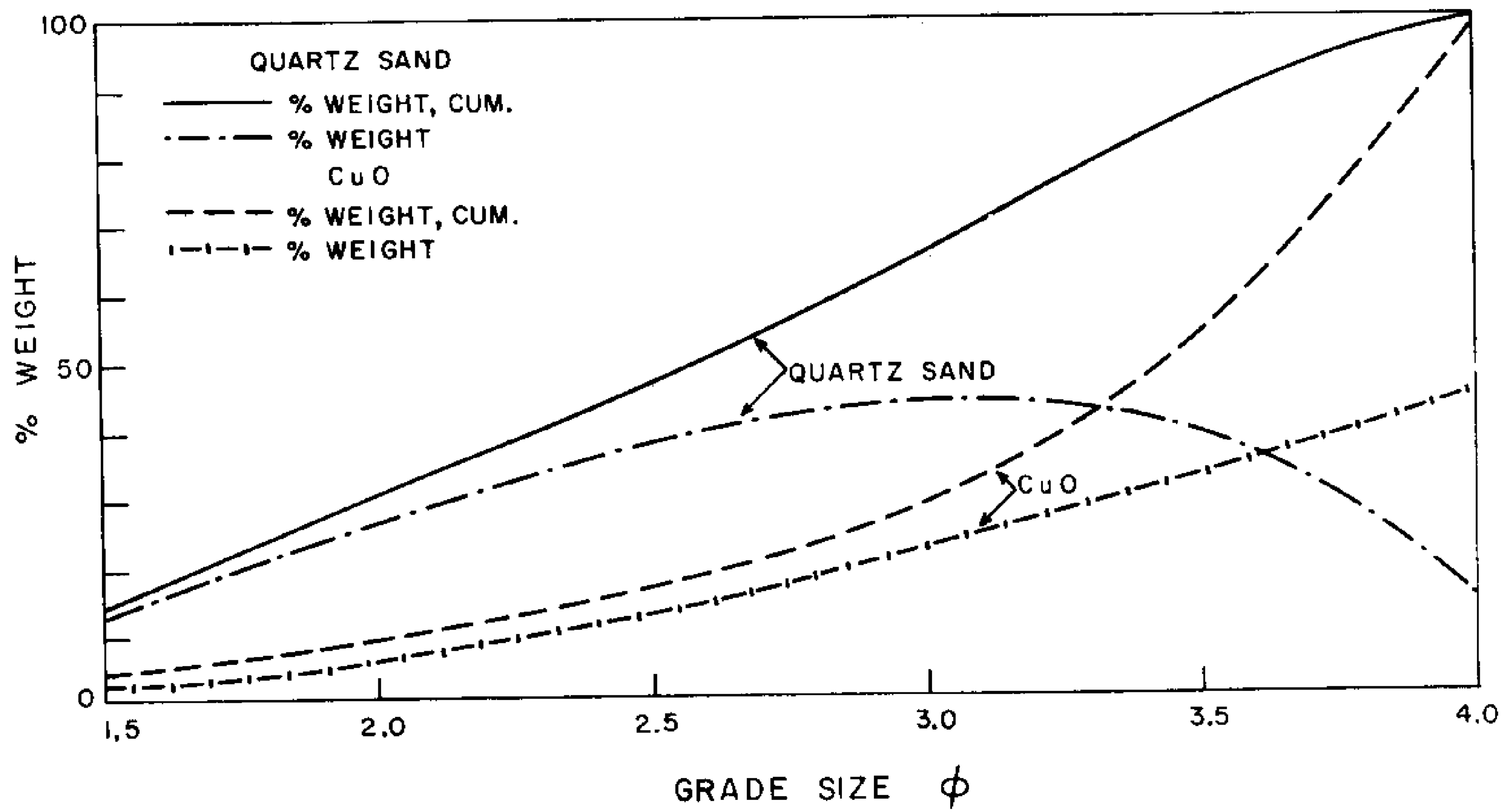

Fig. 4. Procedure for the construction of the artificial models.

1. Clay disk
2. Components for figure mixture (clay, sand, CuO).
3. Creating figure with electro-osmotic knife.
4. Preparing disk to receive figure.
5. Figure inserted into disk.
6. Disk restored to shape.
7. Electro-osmotic cutting ring in place.
8., 9. Excess material trimmed from cutting ring. Sides and ends.
10. Cutting ring with model ready for insertion into PVC liner.

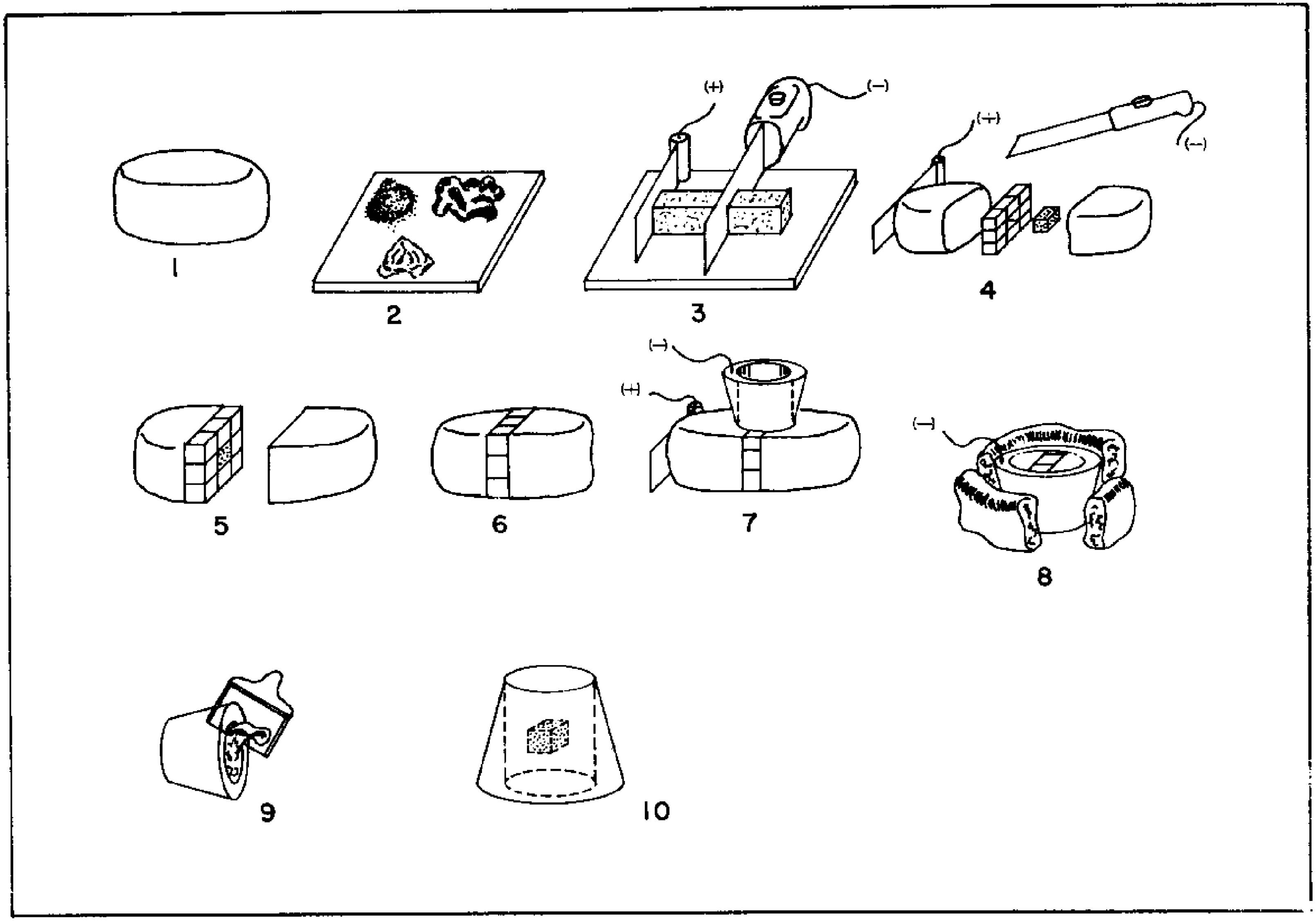
1
2
(+)
(−)
3
(+)
(−)
4
5
6
(−)
(+)
7
(−)
8
9
10

(8) After the model was isolated and the cutting ring trimmed of surplus clay, the general procedure for preparing models for consolidation was followed (see Fig. 1).

Natural models

The natural models consisted of unconsolidated natural macrostructures taken from cores and subjected to the same conditions of consolidation as the artificial models. (These macrostructures are described as models because they were removed from their natural environment and consolidated under artificial conditions.) Core samples collected and examined for the natural macrostructure model part of this study include the following:

(1) Corpus Christi, Texas area, including Padre Island (high energy open beach and washover fans), Osa Bay (low energy, shallow bay with limited circulation), Corpus Christi Bay (medium energy, medium water depth, subject to storm waves), Nueces Bay (shallow, low energy bay with fair circulation and several types of entering drainage, subject to storm waves), and the Nueces River (a mature river entering Nueces Bay at grade).

(2) Northwestern Gulf of Mexico (shelf environment). (Cruise 68-A-6, Texas A&M University R/V ALAMINOS). Five Flexible Liner cores (deep water) collected.

(3) East Bay, Mississippi Delta (interdistributary bay). (Cruise 68-A-14, Texas A&M University R/V ALAMINOS). Three Flexible Liner cores (deep water) and four gravity cores collected.

Locations were chosen in an effort to accumulate samples from a number of different environments of deposition.

The general procedure for processing these samples consisted of the following:

(1) With few exceptions, all cores were sealed as soon as recovered, marked for identification, and transported to the laboratory at Texas A&M University with as little disturbance as possible. The exceptions were the gravity cores which had to be extruded on-board the ship and then packaged.

(2) The cores were removed from their packaging and placed in PVC half-rounds. This was accomplished by extruding the Shelby Tube cores. The Flexible Liner cores were easily slid out of their transport tubes onto the PVC half-rounds.

(3) Electrical logs were run on each core and zones of interest (probable macrostructure concentration) noted.

(4) Whole-core photographs were taken of the core surface.

(5) Whole-core X-ray radiographs were made.

(6) The cores were cut in half longitudinally with an electro-osmotic knife. Each half was consigned to its own PVC half-round.

(7) Half-core photographs were taken of the cut surface of the core.

(8) Half-core X-ray radiographs were made.

(9) Macrostructures were selected from the cores based on visual appearance, X-ray radiographs and electrical logs.

(10) Sections containing the selected macrostructures were removed from the core halves. The two halves of each structure were carefully rejoined to form a cylindrical sample. The use of the

electro-osmotic knife in cutting the cores resulted in disturbance-free surfaces that could be rejoined with no visible change in the structures.

(11) Steps (1) through (8) of the general procedure for preparing models for consolidation were followed (see Fig. 1).

(12) After the post-consolidation radiographs were made, the consolidated models were extruded from the PVC liners, sectioned, compared to the radiographs, and photographed.

(13) The models were reassembled, packaged, marked and stored.

(14) The remaining core material was packaged, marked and stored.

When preparing the natural models for consolidation, 1/4 in. thick porous stones supported by 1/4 in. thick perforated aluminum disks were used in place of the usual 3/4 in. porous stones. This afforded the use of a larger sample (1 3/8 in. high instead of 7/8 in.). Also, "O" rings set into the edge of the aluminum helped to prevent the loss of material by extrusion during consolidation. (Four models had their top stones tilt while being consolidated, but none lost material).

DISCUSSION OF RESULTS

The number of material combinations possible for use in the geometric models is seemingly endless. For one combination of clay and sand it would be necessary to take at least one model type (possibly several) and test it repeatedly. In one test series the moisture content of the figure would vary. In another, the moisture content of the matrix would vary. A third would allow both to vary. Also, the direction of drainage from the cylinder would have to be considered. A change from two directions of drainage to one direction could influence the test results. The orientation of the figure with respect to the direction of drainage would be an additional variable. All series should be repeated for various load values. This procedure could result in enough information to allow the design of a mathematical model.

For the purposes of this investigation it was decided to use one combination of clay and clay-sand figures with a constant moisture content and consolidating load that would serve to demonstrate the concept of model comparison. The materials were chosen on the following basis. First, materials possessing the desirable handling characteristics. Second, the combination with sufficient X-ray density contrast[1] to make possible the necessary radiographs. Third, previous

[1]The combination of clay, fine-grained quartz sand, and CuO provides satisfactory contrast on the X-ray radiographs. However, detail losses of 20% and higher may be expected during reproduction and printing. This represents a serious loss of basic data, therefore, emphasis has been placed on drawings made from the original radiographs.

experience with natural macrostructures indicates that the combination used frequently occurs in nature. Four models, (19 through 22) were fabricated from a second combination of materials (clay with clay-CuO powder mixed and clay with clay coated with CuO powder). Results of the consolidation of these models indicates that the changes induced in a specific figure will be influenced by the materials used in the model.

The changes induced in the natural models varied considerably. In four of the thirteen models the top porous stone was tilted during consolidation but no material was extruded. This is interpreted as indicating a differential consolidation and possible lateral shift of material. The amount of correlation between events observed in the artificial models and those in the natural models appears to be directly related to both the degree of similarity of materials involved and the geometric shapes.

The use of consolidometers imposes a physical condition that must be considered when looking at the results of this study. The upper and lower surfaces of the models were in contact with rigid, porous stones during consolidation. This created two effects. First, the models were allowed to drain in two directions. Second, the rigid stone surfaces created boundary drag which resisted lateral shifting of the model material. The approximate natural analog of the model in the consolidometer would be a soft clay layer between two porous sand layers. Such conditions have been observed in cores recovered in shallow water. The walls of the PVC liners had little apparent effect on the consolidation-induced changes.

Practical considerations caused some minor deviations from ideal test procedures. In making the artificial models, small imperfections occurred due to mismatched cutting angles. Slight distortion by handling was introduced in some natural models during removal from the cores and placement in the PVC liners. (In neither case were the models apparently altered sufficiently to effect the test.) The practice of making the X-ray radiographs immediately prior to and following consolidation precluded the possibility of unknown changes being introduced by handling techniques.

A short period of time was required to load the consolidometers to the 32 TSF maximum. Experience showed that machine and model failure could be significantly reduced by applying the load over a 15 to 30 minute period. This had no perceptible effect on the test results since only the end point of primary consolidation for the maximum applied load was needed. In all tests this point was reached between 65 and 260 minutes after application of the load. The models average an approximate 25% reduction in volume due to consolidation. Figure 5 represents the load response curves for the consolidation tests. The dial indicator readings, adjusted to the same reading at the end point of primary consolidation, represents the reduction in model height in response to the 32 TSF load with respect to time. Elapsed-time-after-loading is shown on a logarithmic scale. The

Fig. 5. Load response characteristics for the consolidation tests. The individual curves have been adjusted to uniform dial reading at the end point of primary consolidation (0.1750 in.) for the applied load. The shaded envelope includes all tests. The solid curve starting at 0.3800 in. is representative of the response curves. All of the tests reached the end of primary consolidation for the 32 TSF load between 65 and 260 minutes after load application.

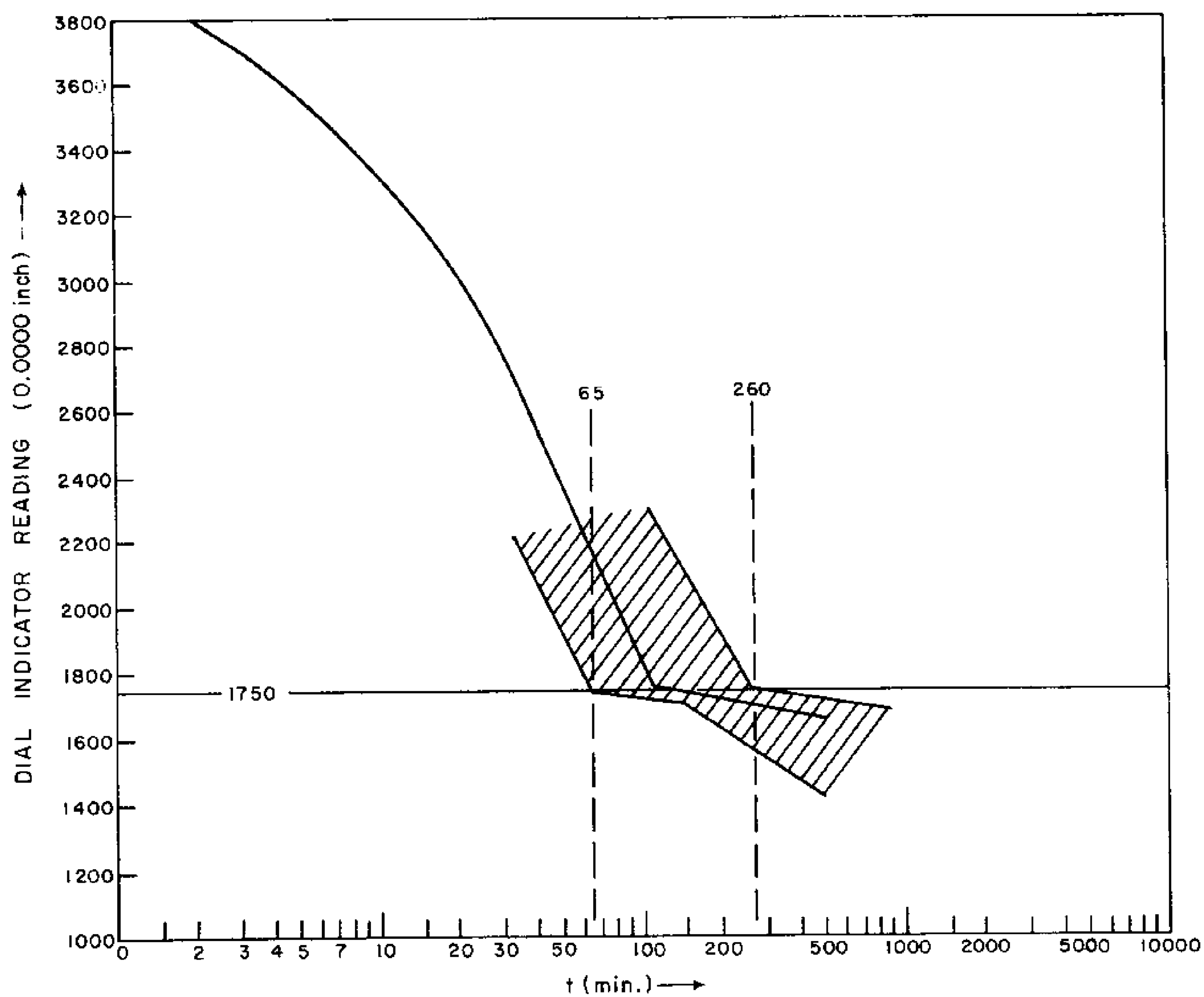
DIAL INDICATOR READING (0.0000 inch)
3800
3600
3400
3200
3000
2800
2600
2400
2200
2000
1800
1600
1400
1200
1000
1750
65
260
0
2
3
4
5
7
10
20
30
50
100
200
500
1000
2000
5000
10000
t (min.)

shaded envelope includes the load curves about the end point of primary consolidation for all tests run. This point was identified on the curves as the intersection of tangents drawn to the limbs of the curve in the vicinity of the marked reduction in slope of the curve. This change in slope occurred when excess pore water pressure approached zero (TAYLOR, 1948). The general trend of the load curves is represented by the solid line extending from the 0.3800 in. to the 0.1700 in. dial reading. Differences in the characteristics of the models are reflected in the shape of the envelope.

In a number of tests failure occurred when the top porous stone became tilted during loading and allowed the model to be extruded from the consolidation cylinder. When this occurred, the test was terminated. However, the model was subjected to post-consolidation X-ray radiography and recovery. Extrusion during consolidation approximates, in some cases, the type of distortion expected when there is a sudden unidirectional release of horizontal confining pressure in natural sediments (i.e., areas bordered by faults, slump blocks, storm channels, and etc.). Certain model runs were repeated as many as four times before a satisfactory test was concluded. All geometric models deemed necessary to the study were run until successfully tested in the consolidometers.

Electrical logging proved to be both a practical and unique technique for locating zones of macrostructures in the cores. All of the cores processed during the course of this study displayed a close relationship between occurrence of macrostructure within an interval and the complexity of the electrical log traces over that interval. The resistivity curve was more sensitive to the changes in lithology that suggested the possible presence of macrostructures. Both a high rate of change and a large magnitude of change in resistivity were found to be indicative of macrostructures. The same criteria were applied to the S.P. curve but with less success. This was probably due to a low level of S.P. variation along the core and a lack of sensitivity in the instrument used. These relationships were confirmed by X-ray radiography and visual observations of cut cores. In several cases the electrical logs indicated the presence of structures not seen on the X-ray radiographs but quite apparent when the cores were cut.

Artificial models

Figure 6 represents the results of consolidation tests made with artificial geometric macrostructure models. Thirty-five separate models were tested in order to complete the series. Models 1 through 17 consist of clay with clay-sand figures. Models 19 and 20 were composed of clay with clay figures whose surfaces were coated with CuO powder. Models 21 and 22 had figures of clay mixed with CuO powder. In Fig. 6 representation on the left side of the page depicts the model prior to consolidation. The drawings on the right represent the model after consolidation. These drawings were made from stereo

Fig. 6. Artificial geometric models of macrostructures prior to and following consolidation.
The left column of drawings represents pre-consolidation models.
The right column of drawings represents the same models in the post-consolidation condition.
All of the drawings were made from stereo X-ray radiographs.
The numbering code consists of alternating letters and numbers as follows:

1. Prefix "C" denotes post-consolidation. Lack of the prefix indicates pre-consolidation.
2. First numeral is model number.
3. Letter following first numeral indicates model orientation. Orientation "A" is understood if no letter follows the first numeral.
4. Second numeral is the run or edition of the model.

Example: C9-3: post-consolidated condition of model 9 in the "A" orientation, third edition.
12B : pre-consolidation condition of model 12 in the "B" orientation, first edition.

Models 1 through 17 are clay with clay-sand figures. Models 19 and 20 are clay with flay figures coated with CuO. Models 21 and 22 are clay with clay figures mixed with CuO. The stipplings represent the clay-sand mixture.

1

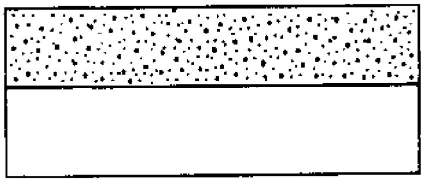

C1

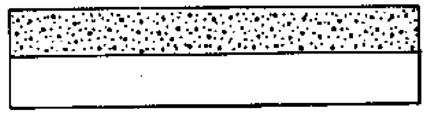

2

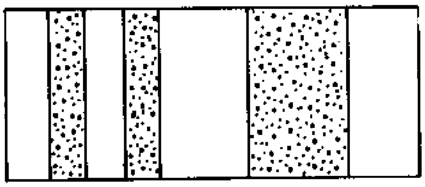

C2

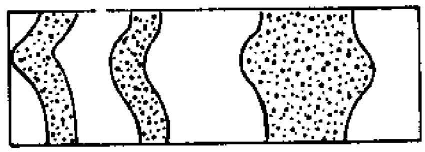

2-2

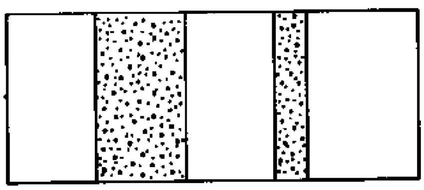

C2-2

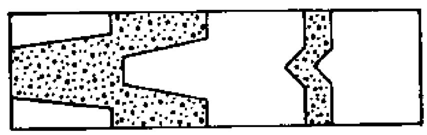

3-3

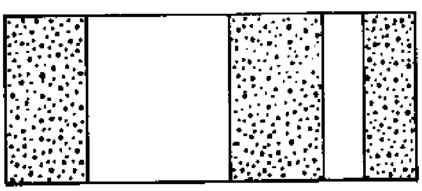

C3-3

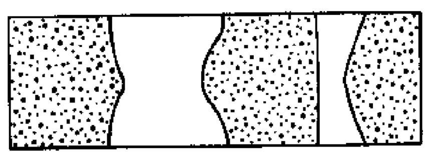

4

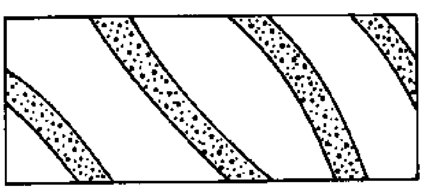

C4

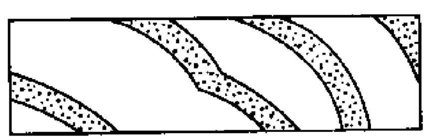

5

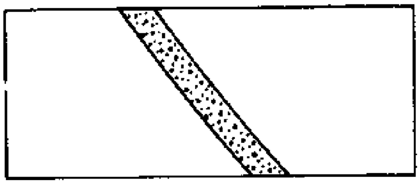

C5

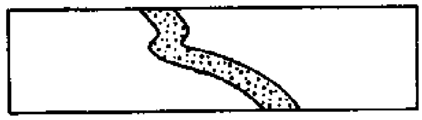

6

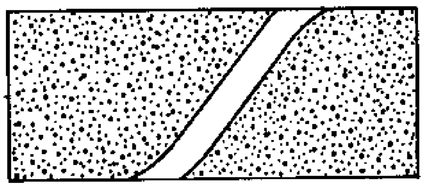

C6

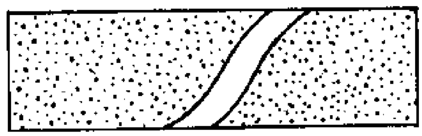

7

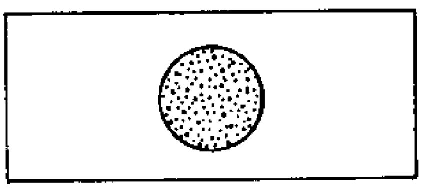

C7

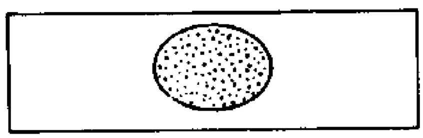

8

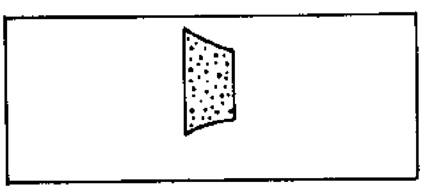

C8

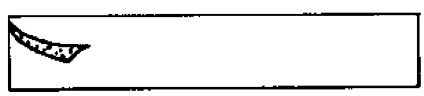

8B

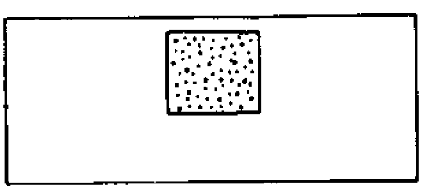

C8B

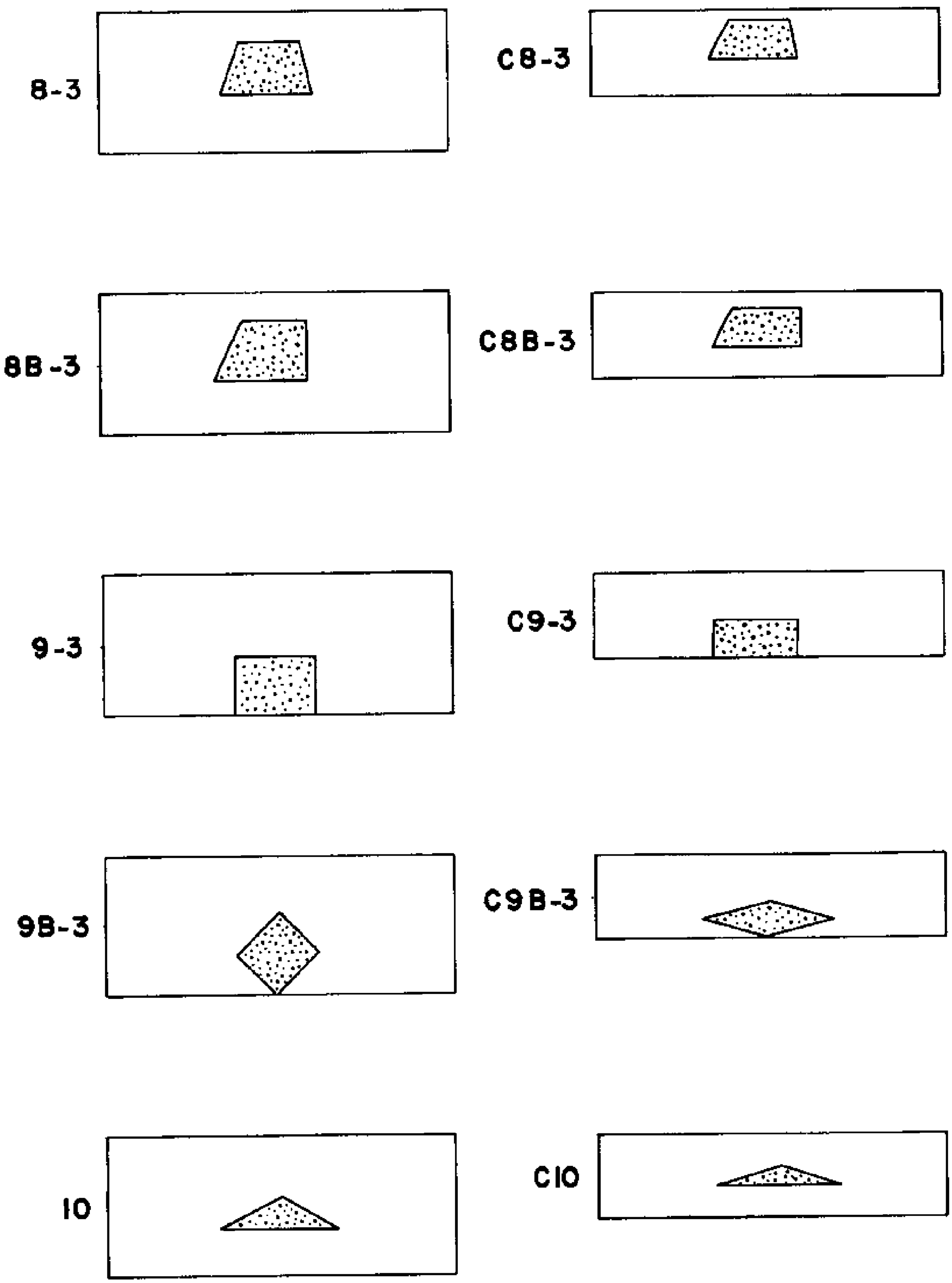
8-3
C8-3
8B-3
C8B-3
9-3
C9-3
9B-3
C9B-3
10
C10

11

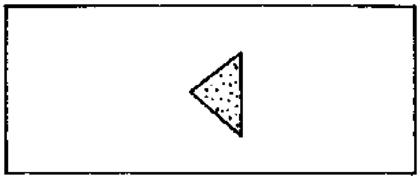

C11

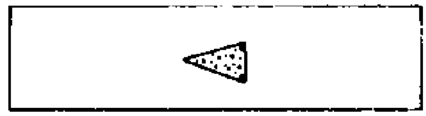

11B

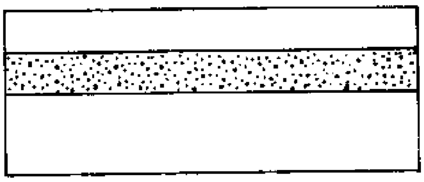

C11B

12

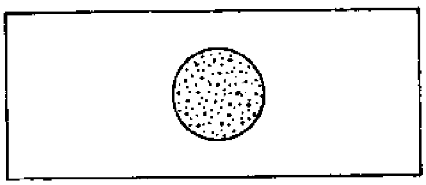

C12

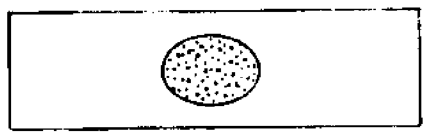

12B

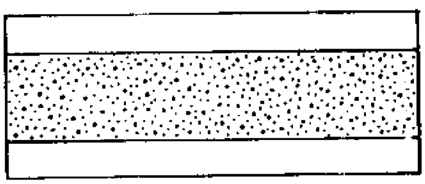

C12B

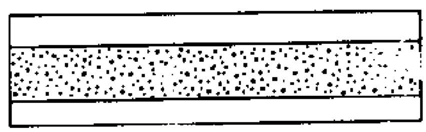

13

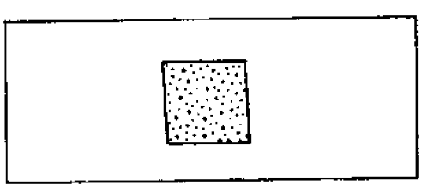

C13

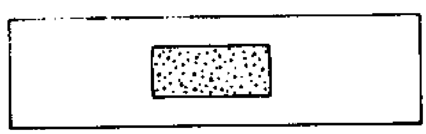

13B

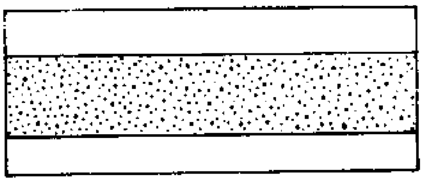

C13B

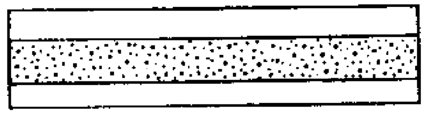

14

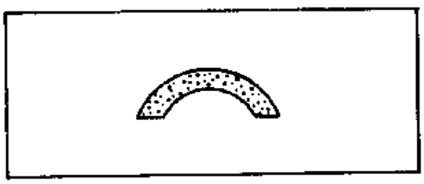

C14

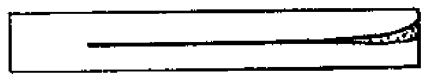

14B

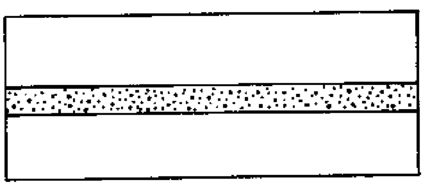

C14B

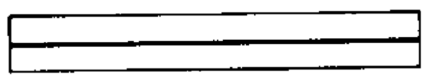

15

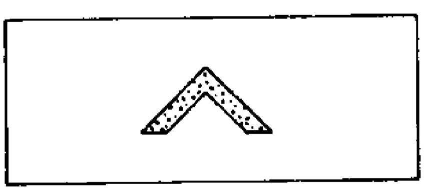

C15

15B
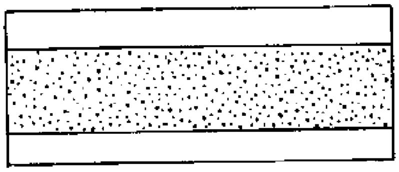

C15B
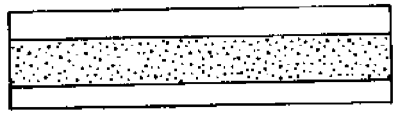

16
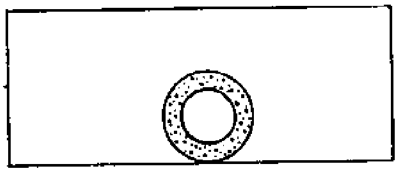

C16
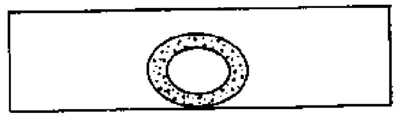

16B
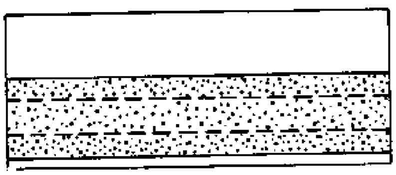

C16B


17
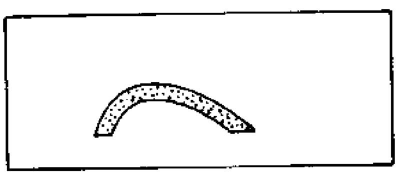

C17
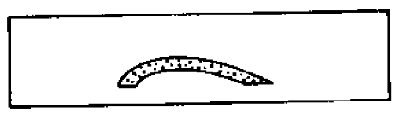

17 B
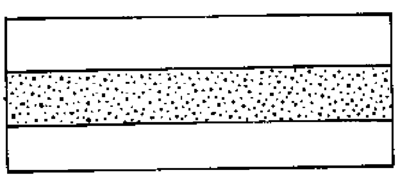

C17B
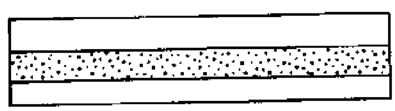

18

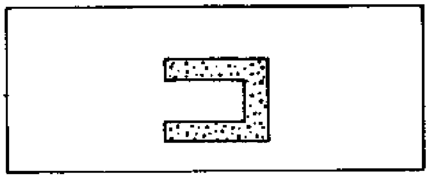

C18

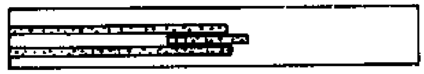

18B

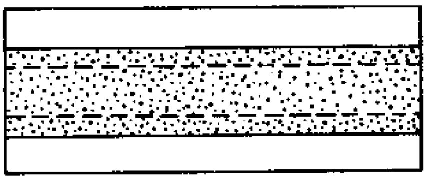

C18B

19

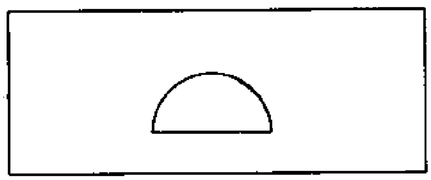

C19

19B

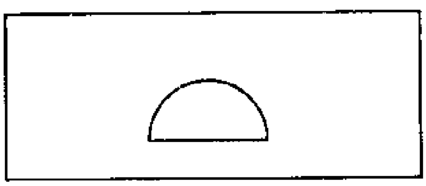

C19B

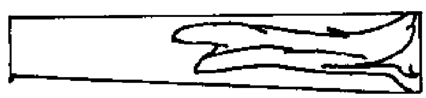

19C

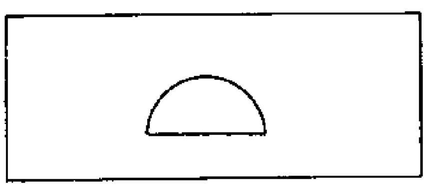

C19C

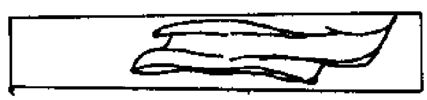

20

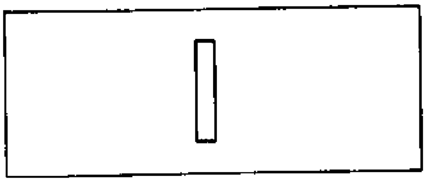

C 20

20B

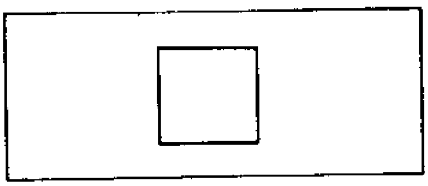

C20B

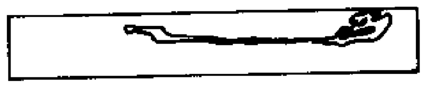

21

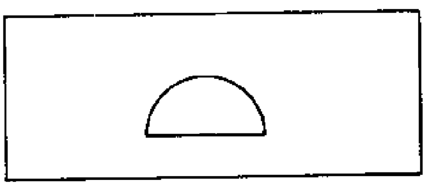

C 21

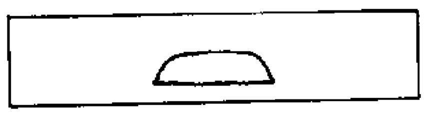

22

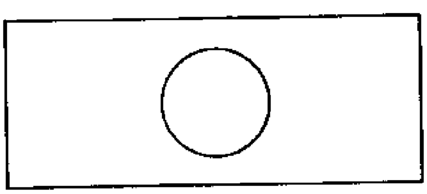

C 22

X-ray radiographs.

The following comments apply to the models illustrated in Fig. 6 .

Model 1. Two horizontal layers. No consolidation-induced distortion is apparent.

Model 2. Alternating vertical layers of various thicknesses. The bulging middle of the thick clay-sand layer in drawing C2 indicates a relative reduction in volume of the clay. The top and bottom of the layer have not changed width during consolidation. This is due to the influence of the rigid porous stone boundaries. The two thin sand layers may have bent (1) in response to the clay deformation caused by the thick layer bulge, or (2) because the layers are thin enough to preferentially respond to load by bending instead of bulging.

Model 2-2. Two vertical layers of different thickness. Extrusion occurred during consolidation (material escaped to the left). Note the influence of the rigid surface boundaries. The sharp angles and straight lines are possibly due to explosive release of pressure.

Model 3-3. Three vertical layers, two in contact with the cylinder walls. The clay-sand layers bulge at the expense of the clay. Influence of the rigid boundaries is apparent. The right-hand clay-sand layer was prevented from expanding to the right and consequently bulged considerably to the left. This expansion was taken up in the thin clay layer but force transmitted horizontally apparently prevented the right side of the center layer from expanding to the right (Fig. 7). Both thick clay-sand layers bulged into

Fig. 7. Stereo X-ray radiograph of model number 3A3.
A. Pre-consolidation
B. Post-consolidation

3A3

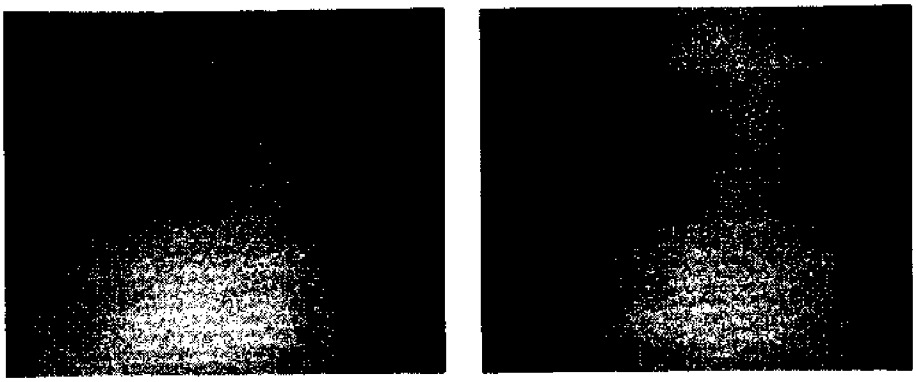

A

B

the intervening clay which was thick enough to accomodate them.

Model 4. Alternating layers dipping roughly 45°. Note (1) an increase in curvature of all layers, (2) a trend towards flattening of the dip, and (3) the reversal of curvature and break in the left-middle clay-sand layer.

Model 5. Single layer dipping approximately 45°. There is a tendency to flatten the dip more in the center than at the top and bottom (due to the rigid boundary). The resulting center elbow or break may be due to the differences in mobility of the clay at the middle and top and bottom. This sample was not extruded and there was no migration of center material out of the cylinder (Fig. 8).

Model 6. Single clay layer at approximately 45°. There is a steepening of the center part of the layer which results in a more distinct "S" shape.

Model 7. Sphere. This figure has been deformed into a prolate spheroid.

Model 8., 8B. Cube. The figure was extruded almost completely out of the cylinder. The irregular shape of the pre-consolidated figure as seen in the A orientation was caused by improper fabrication. Extrusion proceeded from the upper left of the model when viewed in the A orientation. In the B orientation the top of the extruded figure appears sharp and parallel to the upper surface. This is due to the boundary effect of the top porous stone. The

Fig. 8. Stereo X-ray radiographs of model number 5A
A. Pre-consolidation
B. Post-consolidation

5 A

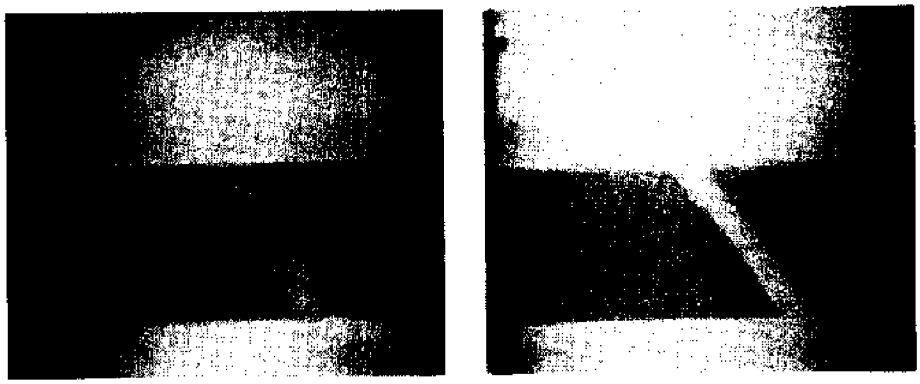

A

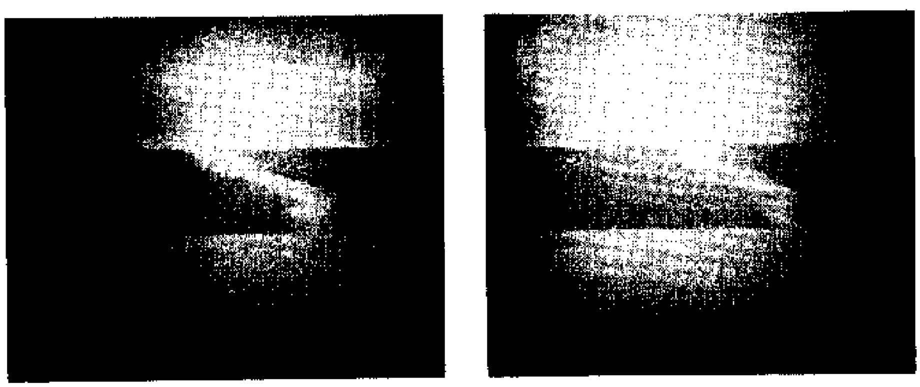

B

bottom part of the extruded figure was subject to slight irregularities of flow as the material extruded and therefore became irregular.

Model 8-3., 8B-3. Cube. Improper cutting angle produced a trapezoid rather than a cube. Consolidation flattened and lengthened the figure without changing the angle of the sides or their straightness.

Model 9-3., 9B-3. Rectangle on edge. This figure was flattened and lengthened in both the A and B views. The angles were not changed in the A view but changed considerably in the B view. None of the sides were distorted. Although the edge of the figure touches the bottom stone, it does so in the center and only along a thin line. This prevented any apparent boundary influence.

Model 10. Pyramid. This figure was flattended and lengthened with no apparent distortion of its sides.

Model 11., 11B. Triangular rod. The figures show a flattening and lengthening without distortion of edges. The B view indicates no apparent influence by the cylinder walls.

Model 12., 12B. Circular rod. The rod flattened into a spheroidal section. The B view shows a reduction in thickness of the figure without distortion of the sides. The ends apparently have not been effected by the cylinder walls.

Model 13., 13B. Square rod. This figure was flattened into a rectangular shape in the A view. The B view indicates neither edge distortion nor influence of the cylinder wall.

Model 14., 14B. Symmetrical arch. Extrusion has occurred to the right in the A view. There is an accumulation of figure material at the point of extrusion. The A view also shows that some figure material migrated to the left against the direction of extrusion.

Model 15., 15B. Triangular arch. Flattening of this figure was accompanied by a slight concavity of the sides. Neither edge nor end distortion occurred.

Model 16., 16B. Hollow cylinder. The figure was flattened but there was little or no change in the walls. No distortion appears in the B view.

Model 17., 17B. Asymmetrical arch. Distortion in this figure included flattening and a reduction in curvature. The amount of curvature change appears to have been greatest where the arch was steepest (Fig. 9). The B view shows no distortion.

Model 18., 18B. Open rectangular bar on side. Extruded to the left, the figure shows none of the distortion normally caused by such action. Probably, there was only a slight amount of extrusion late in consolidation.

Model 19., 19B., 19C. Clay hemisphere coated with CuO powder. This figure was extruded to the right in the B view. This is an example of differential distortion of clay-clay figures due to horizontal release of pressure. Figure 10 presents the pre-and post-consolidation stereo radiographs of 19B and a stereo pair of radiographs taken parallel to the direction of applied force. It

Fig. 9. Stereo x-ray radiographs of model number 17A.
A. Pre-consolidation
B. Post-consolidation

17A

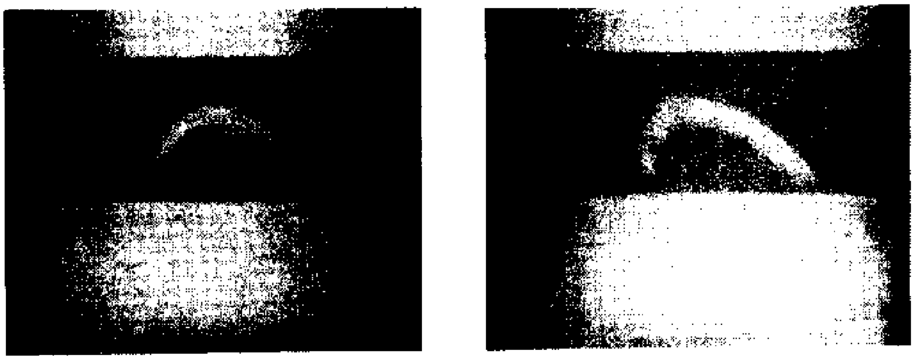

A

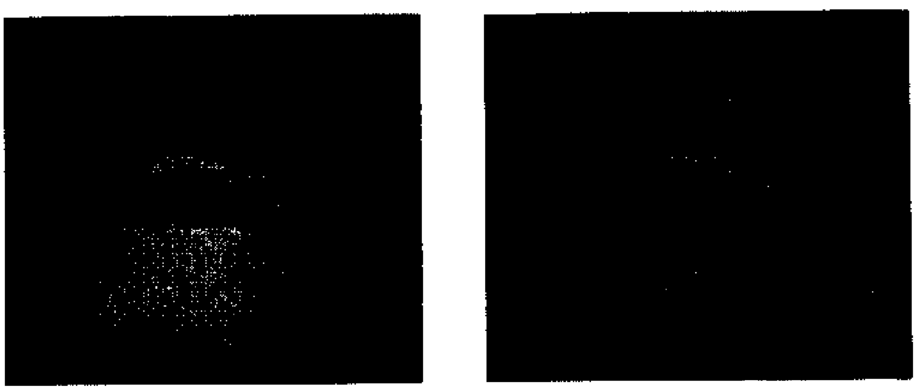

B

Fig. 10. Stereo X-ray radiographs of model number 19B.
A. Pre-consolidation
B. Post-consolidation
C. Post-consolidation. Parallel to direction of applied load.

19 B

A

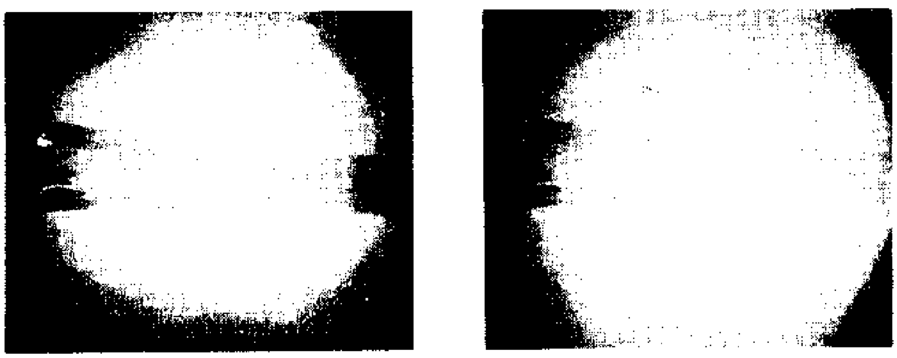

B

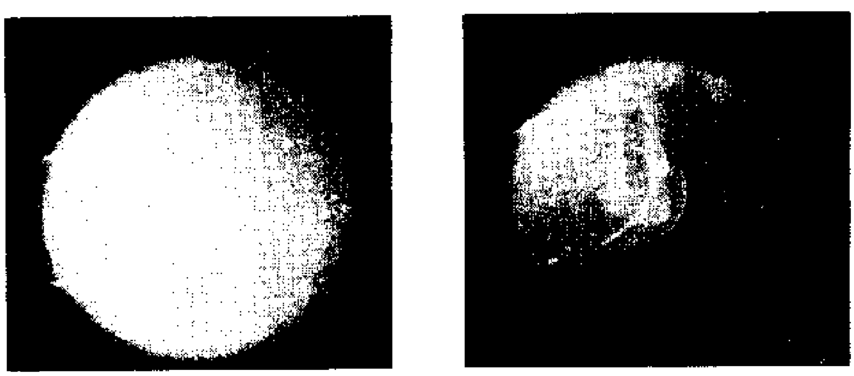

C

should be noted that the distorted figure resembles macrostructures often attributed to biological agents. Also, comparison with a similar clay-sand model (Model 14) suggests a difference in response to horizontal release of pressure. The figure in Model 14 (clay-sand symmetrical arch), extruded in an even plain leaving a small amount of excess material near the place of exit from the cylinder. The figure in Model 19 shows convolutions and distortions of an entirely different nature.

Model 20., 20B. Thin, vertically oriented rectangular plate of clay coated with CuO powder. During extrusion the entire figure was drawn into a single thin string. This suggests a point of extrusion rather than a broad failure to confine the model.

Model 21. Hemisphere of clay mixed with 1% CuO powder. In this figure flattening was accompanied by slight surface irregularities. The amount of flattening is greater than similar models with clay-sand figures (compare with the upper half of the figure in Model 7C).

Model 22. Sphere of clay mixed with 1% CuO powder. During extrusion material from the right side of the figure migrated through the figure leaving sharp contact lines with the figure.

Natural models

The natural models used in this study were selected from cores collected from a number of different environments. Electrical logging and X-ray radiography were used to locate core sections having the greatest concentration of useable macrostructures. The cores selected were photographed, cut in half longitudinally, and re-photographed. Half-core X-ray radiographs were made and a final selection of models noted. Figures 11 and 12 summarize the use of electrical logging, X-ray radiography and electro-osmotically cut cores in the selection and preparation of the natural models.

The core was a long Shelby Tube core (68-NB-Station 7) collected at the partially-abandoned mouth of the Nueces River. The whole-core photograph illustrates the lack of structural information present on the core surface. The thin, dark trace down the length of the core was made by an electrical logging electrode.

Both the spontaneous potential and resistivity curves of the electrical log indicate a response to the presence of lithologic changes and macrostructures. The S.P. curve recorded only small differences in potential along the core. (The sandy zone between 18 and 21 ins. caused a weak but definite response.) The resistivity curve, on the other hand, clearly indicates the location of the resistive sand layers (6.5 to 7.5 in., 10.25 to 10.75 in., 16 to 16.5 in. and 18 to 21 in.). In addition, clay layers and combination layers can be identified. Comparison of the electrical log with the half-core photograph indicates the meaning of the electrical curves in terms of core lithology. The X-ray radiograph confirms the prominence of the macrostructures located visually and on the electrical logs and furnishes information about their internal shape.

Fig. 11. Natural model selection procedure - general. Electrical logs made on the whole core are used to locate probable concentrations of structures within the core. X-ray radiographs and the electro-osmotically cut core are compared with the electrical logs.

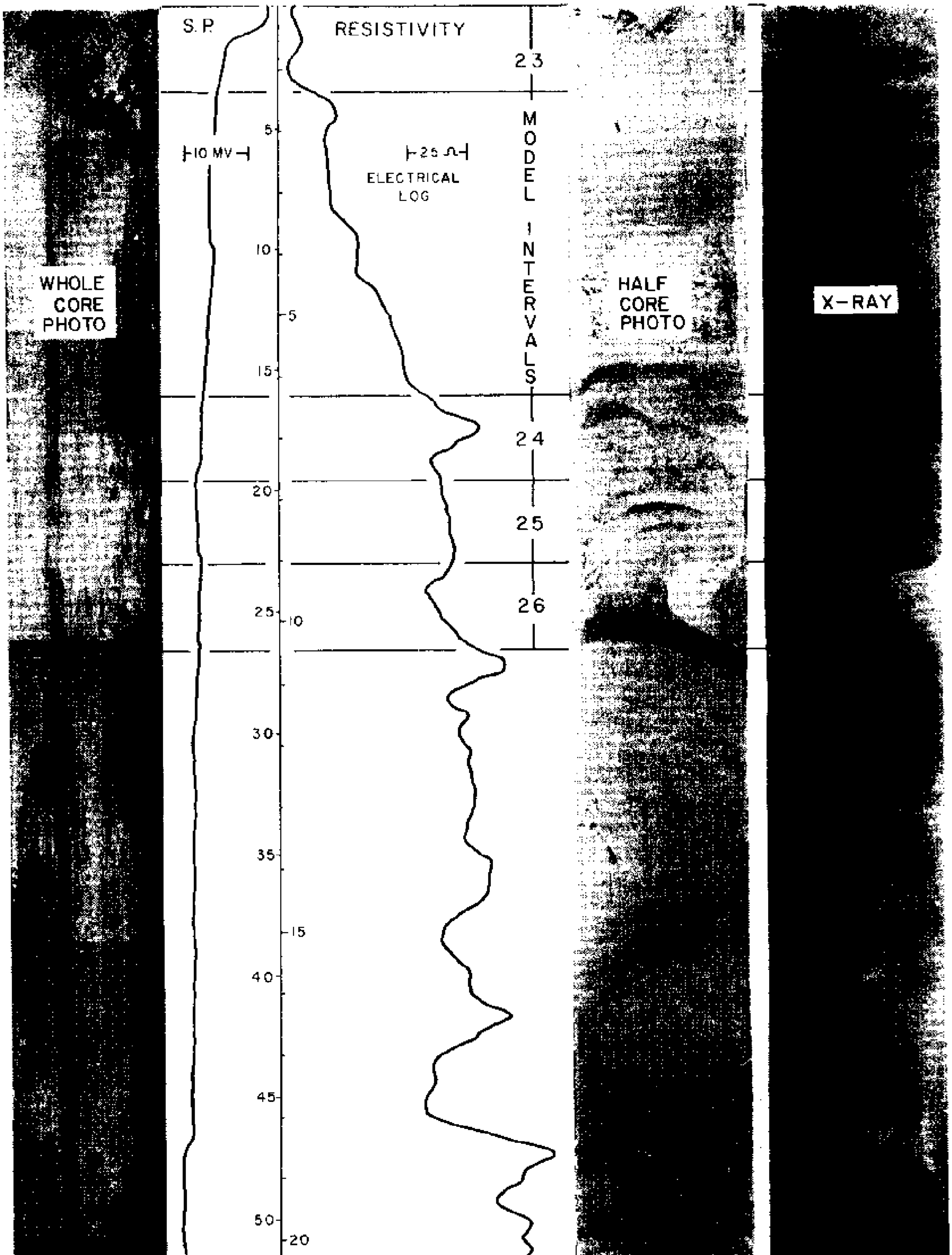

WHOLE CORE PHOTO
S.P.
10 MV
RESISTIVITY
25 Ω
ELECTRICAL LOG
MODEL INTERVALS
23
24
25
26
HALF CORE PHOTO
X-RAY
CM
IN

Fig. 12. Natural model selection procedure - specific. (Enlarged view of upper part of Fig. 11).
Careful inspection and comparison of the X-ray radiographs and the electro-osmotically cut cores confirm the suitability of the structures before final selection.

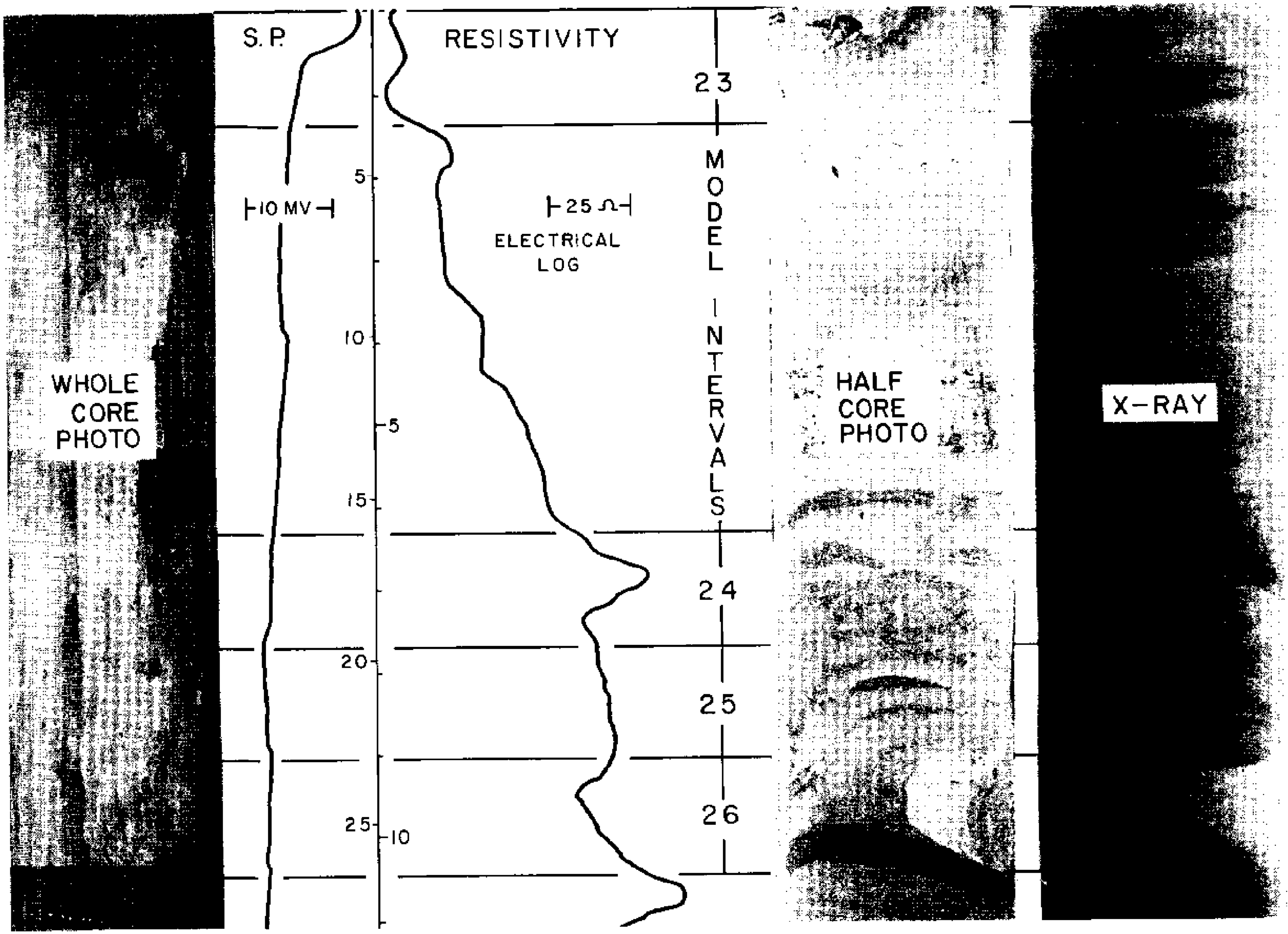
WHOLE CORE PHOTO
S.P.
10 MV
RESISTIVITY
25 Ω
ELECTRICAL LOG
MODEL INTERVALS
23
24
25
26
5
10
15
20
25
5
10
HALF CORE PHOTO
X-RAY

On the basis of this comparison natural models 23, 24, 25 and 26 were selected. Figure 12, an enlarged view of the top part of Fig. 11, presents a more detailed view of the structures selected. The structures chosen were removed from the core halves with the help of the electro-osmotic knife. The two halves were carefully matched and rejoined by pressing them lightly together. The cutting ring was then used and the models fitted into PVC cylinders for X-ray radiography and consolidation.

Figure 13 presents a selection of the pre-and post-consolidation stereo X-ray radiographs of models 23, 24, 25 and 26. In each case the orientation closest to that of the photographs and radiograph of Fig. 12 were used. It is significant that all four of these models are made of materials very similar to that used in the artificial models. Note also that the radiograph in Figs. 11 - 12 is a contact print of the original radiograph. The radiographs in Fig. 13 on the other hand, are prints of photographs taken of the original radiographs. Consequently, when comparing the two, keep in mind that one is the negative of the other.

In Fig. 13 the A pair of radiographs are pre-consolidation, the "B" pair, post-consolidation, and "C" is a photograph of the sectioned consolidated model.

The following notes refer to Fig. 6., Fig. 12. and Fig. 13.

Model 23. The model exhibits differential consolidation attended by a reduction in clay volume (less dark area in B.). Also, the

Fig. 13. Stereo X-ray radiograph of natural models 23, 24, 25 and 26. Model number and orientation designation are at the top of each page.
Stereo pair A is of the unconsolidated model.
Stereo pair B is of the consolidated model.
Photography C is of the sectioned model after consolidation.
Model 25 was destroyed during removal from the PVC liner and not available for post-consolidation sectioning.

23A

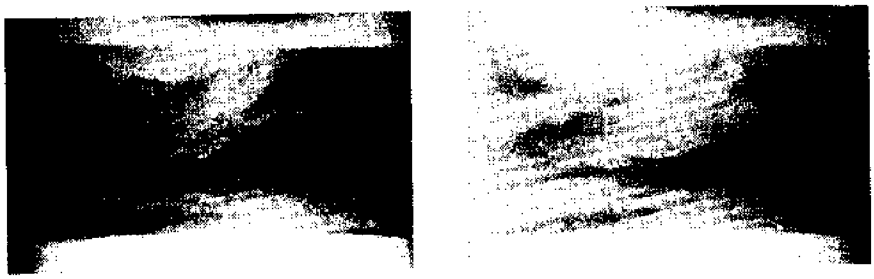

A

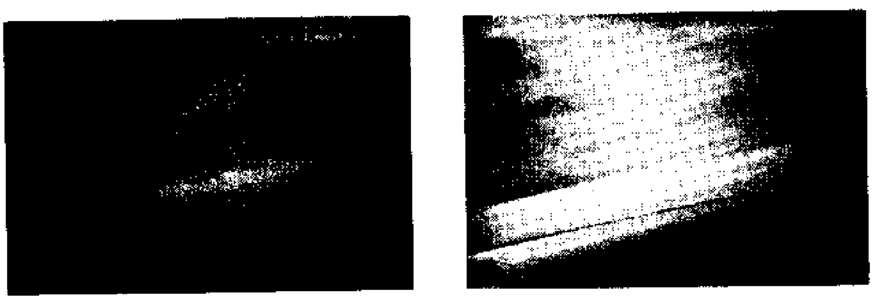

B

C

24C

A

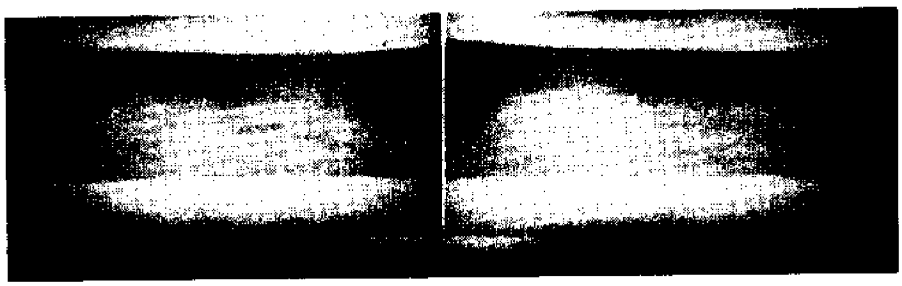

B

C

25C

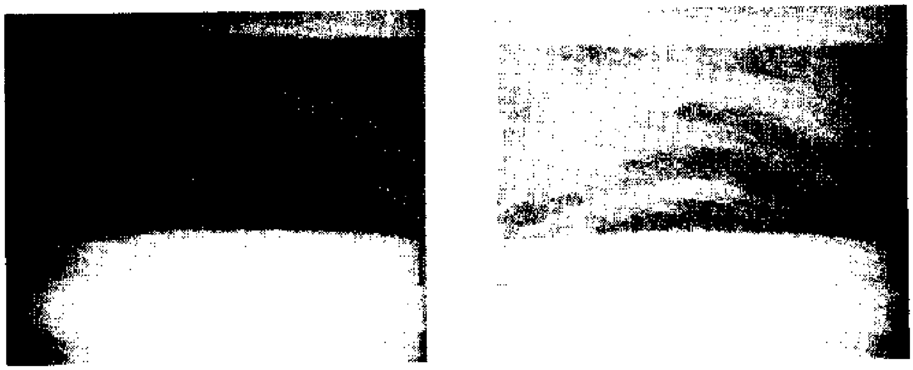

A

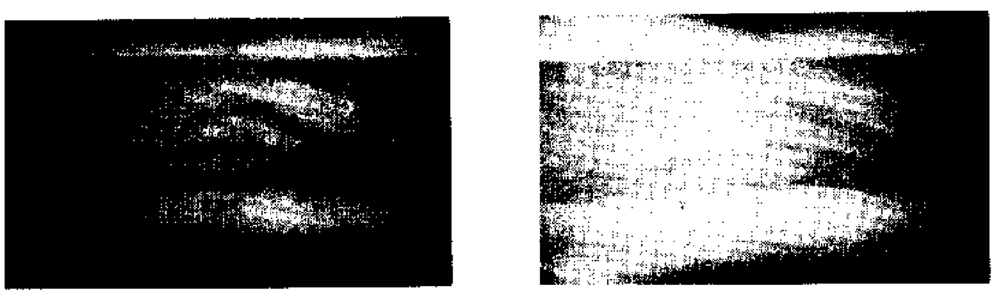

B

26B

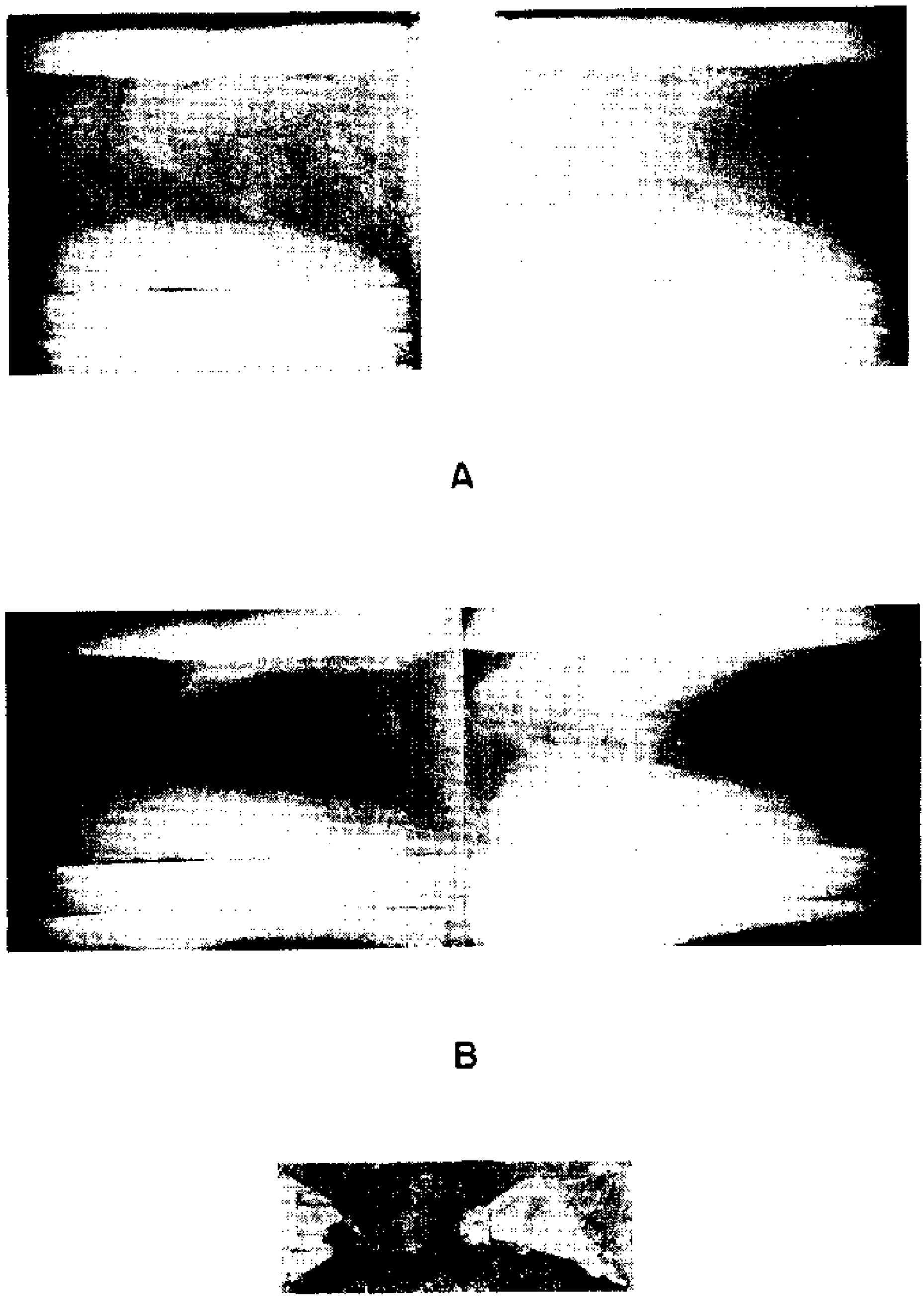

A

B

C

individual layers appear to be more clearly parallel to each other after consolidation. Photograph C is a section of the consolidated model in about the same orientation.

Model 24. This model approaches the conditions of artificial model 17, the asymmetrical arch. Both represent arch-like sand lenses in a clay matrix (see Fig. 12, model interval 24). The consolidation-induced changes in the structures are also similar. The arch in the upper right of model 24C has been flattened by consolidation and reduced in curvature. The prominent sand mass in the lower left quarter of 24C responded to consolidation in much the same way as artificial model 12 (clay-sand sphere). Considering only the upper left quadrent of the figure in model 12, we can see the flat top and steeply curved flank of the once spherical figure. The same type of change is apparent in the lower left quarter of 24C. The photograph of the sectioned model confirms these observations.

Model 25. This model exhibits consolidation-induced changes similar to artificial models 17 (asymmetrical arch) and 4 (alternating layers dipping roughly 45°). The arch in the lower center of 25C is closely approximated by the figure in artificial model 17. The right limbs of the top and middle arches can be compared to the left center layer of artificial model 4. In both cases there was a similar reversal of curvature.

Model 26. This model represents an approximation in nature of the rigid surface condition caused by the porous consolidometer stones in contact with the models. The massive sand at the bottom of the model remains virtually unchanged by consolidation. Note, however, that the clay above it was reduced in volume. The fine structures running through the clay indicate drag along the surface of the sand during consolidation. These fine structures appear to have been concentrated at the expense of the clay in a sharply bent center column during consolidation. Photograph C of the sectioned model shows the lithological differences.

Figure 14 is a collection of drawings representing the X-ray radiographs of the natural models. In this series each page contains drawings of the pre-and post-consolidation radiographs of the A, B, and C orientations. Models 23, 33, 34, and 35 all had their top porous stones tilted during consolidation, but none lost material. Models 23 through 26 have been discussed above and are included here in order to furnish a comparison between radiographs and drawings.

Model 27. This model was taken from the top of core 68-NB-Station 5, a long Shelby Tube core. This was a fan-like structure in very soft, light and dark clay. The structure flattened out during consolidation giving the center a tightly folded appearance.

Model 28. Taken from the middle of core 68-NB-SD1, a short Shelby Tube core, the structure was a nearly vertical worm burrow filled with silty clay and surrounded by a section of firm clay with thin silt layers. The materials in this model approximated those of the artificial models. Consolidation induced a central bulging of the burrow at the expense of the clay. This behavior was very similar

Fig. 14. Natural models of sedimentary macrostructures prior to and following consolidation. The drawings were made from the original X-ray radiographs of the models. Each page contains the drawings of the pre- and post-consolidation radiographs of one model in three orientations. Drawings on the left represent the pre-consolidation condition of the model. The accompanying letters denote the orientation. The solid lines outline prominent trends or features. Stippling indicates sandy or silty material. Hatchers represent areas that are predominantly clay.

A

23

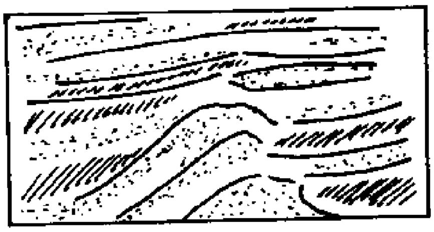

CA

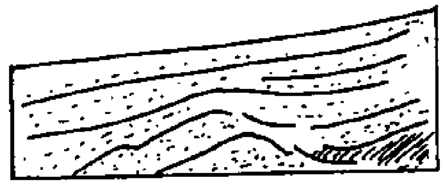

B

CB

C

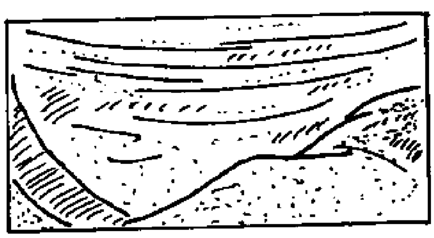

C C

A

2-4

CA

B

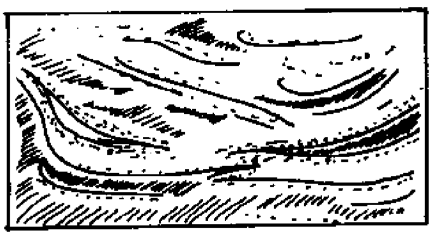

CB

C

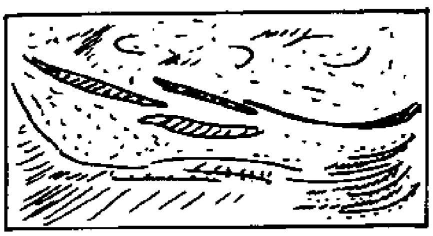

CC

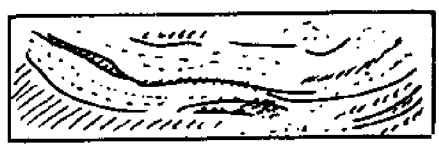

A

25

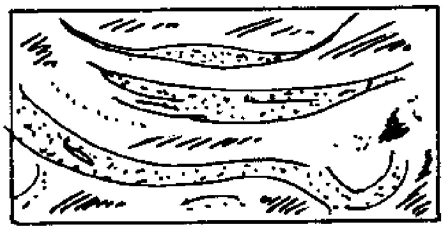

CA

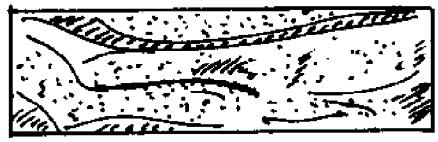

B

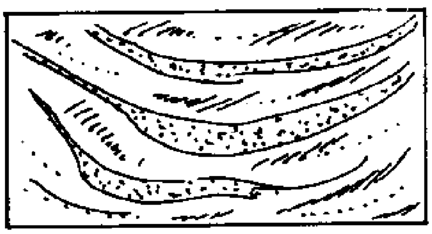

CB

C

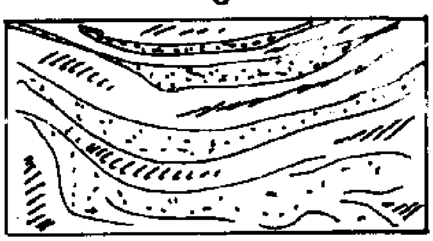

CC

26

A

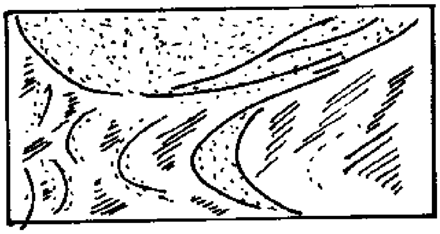

CA

B

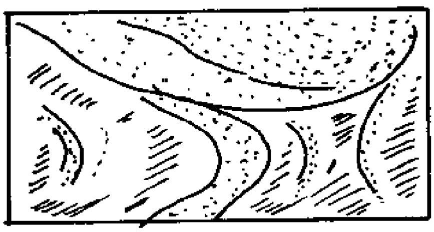

CB

C

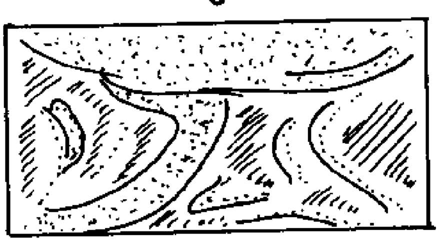

CC

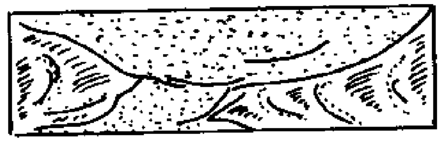

27

A

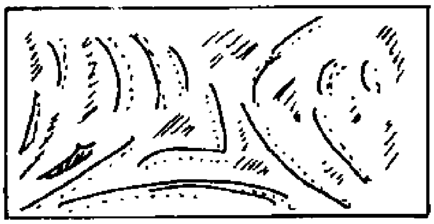

CA

B

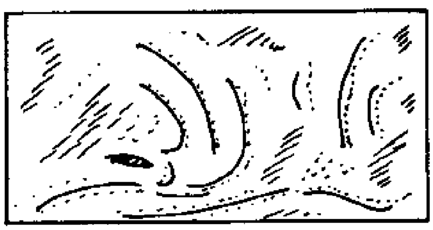

CB

C

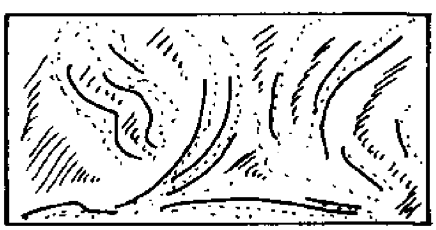

CC

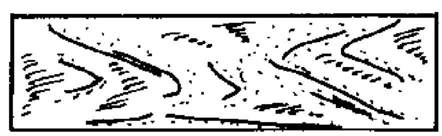

A

28

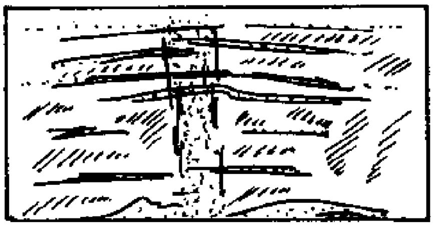

CA

B

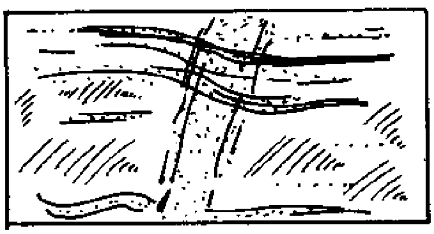

CB

C

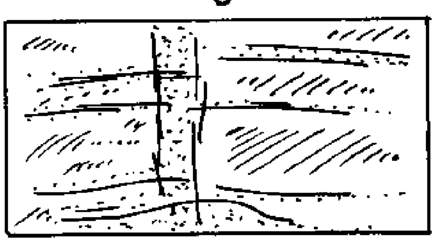

CC

29

A

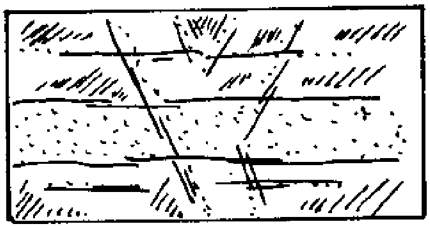

CA

B

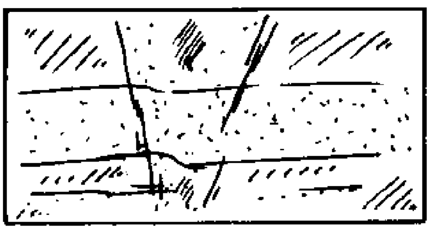

CB

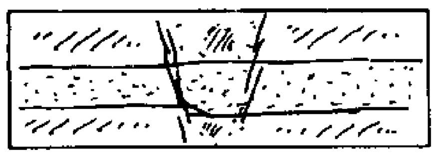

C

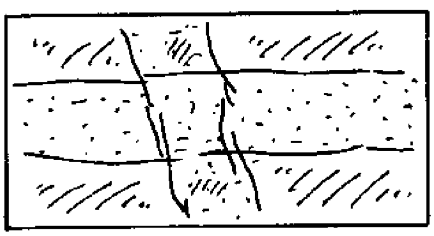

CC

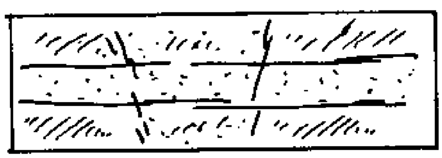

A

30

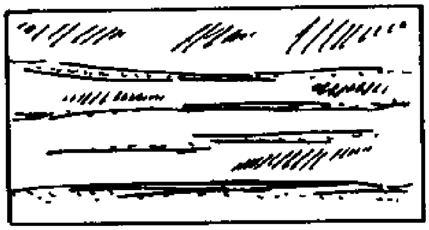

CA

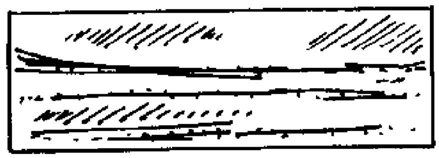

B

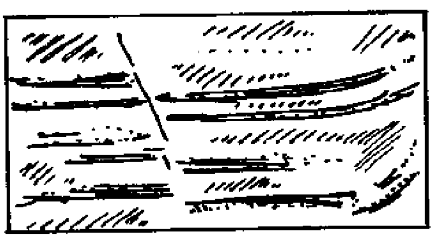

CB

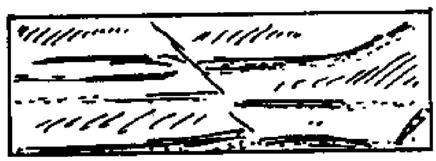

C

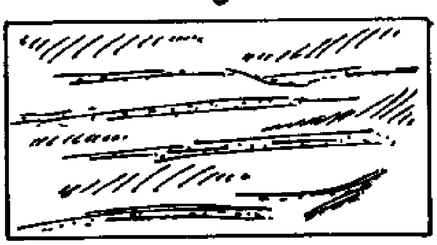

CC

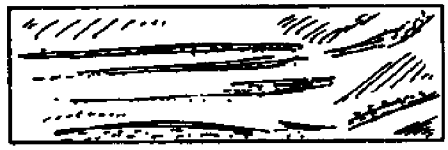

A

31

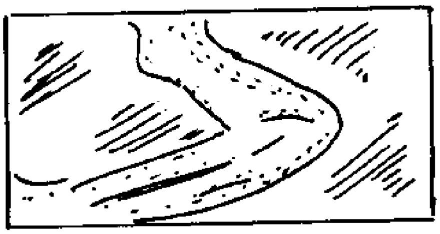

C A

B

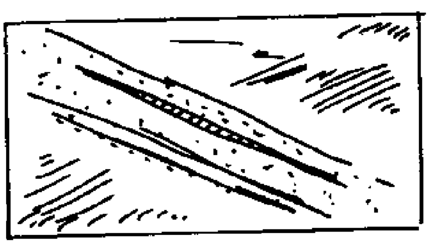

C B

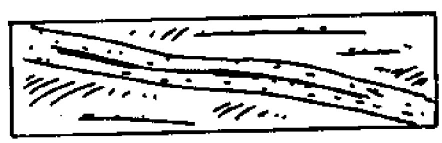

C

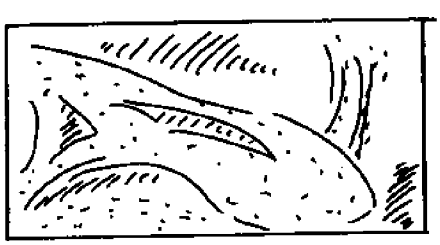

CC

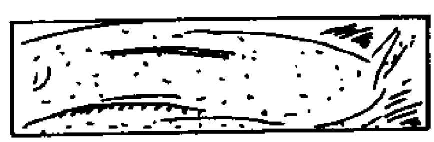

A

32

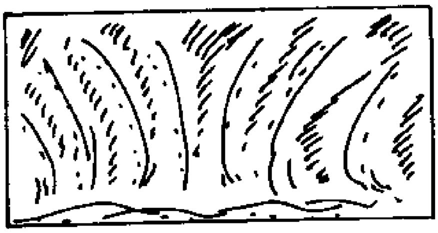

CA

B

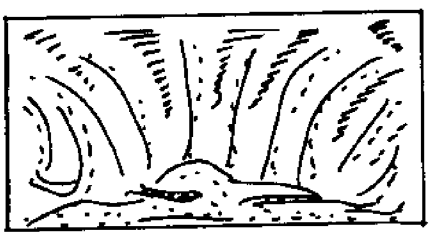

CB

C

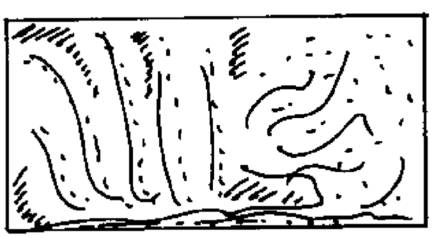

CC

33

A

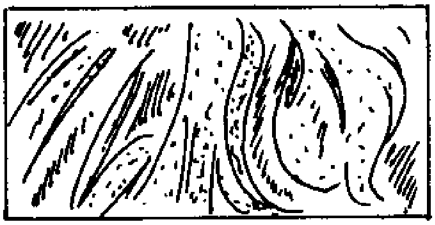

CA

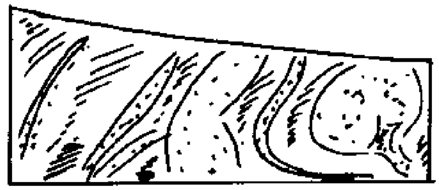

B

CB

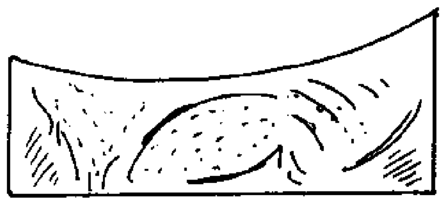

C

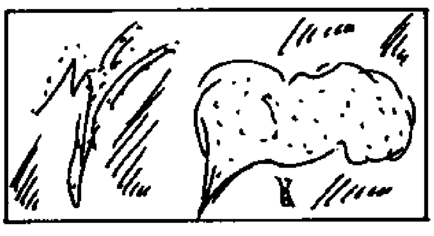

CC

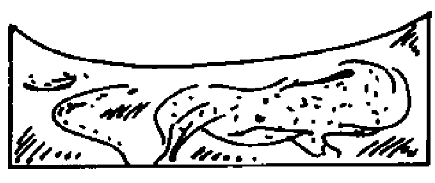

34

A

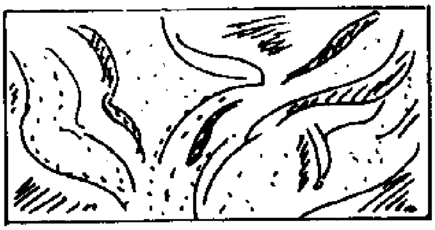

CA

B

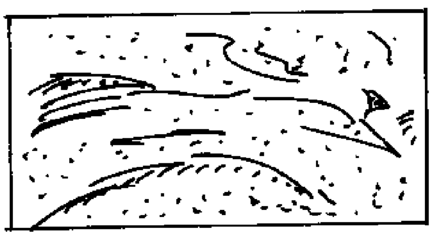

CB

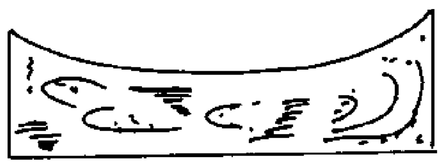

C

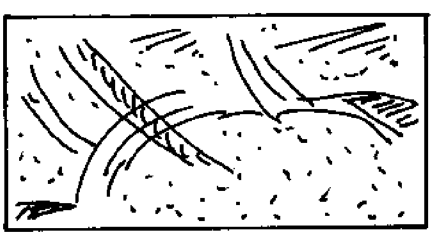

CC

A

35 

CA

B

CB

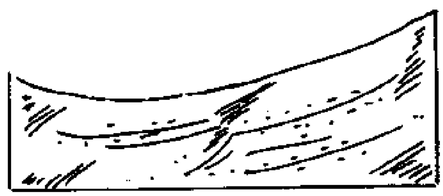

C

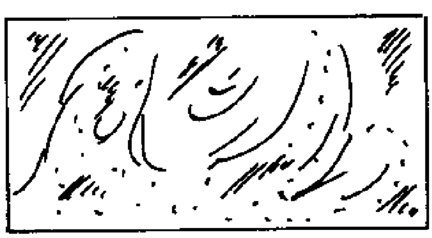

CC

to the results of consolidation seen in artificial model 2.

Model 29. This model was taken from the same core as model 28 but lower in the section. The model is an intersection of two silt-filled burrows surrounded by clay and silty clay. The response to consolidation was similar to that of model 28 but not as pronounced. A central layer of silty clay may have retarded the bulging.

Model 30. This model was taken from the top of core 68-NB-Station 4, a Shallow Water Flexible Liner core. This was a very soft, clay-clay model that displayed macrofaulting. Consolidation-induced changes were minimal. Orientation B afforded a view of the fault. It appeared to have been reduced in apparent dip by consolidation.

Model 31. This model was taken from core 68-NB-Station 4, a long Shelby Tube core. The structure, composed of a sandy clay layer in a clay body was very similar in shape and composition to artificial model 5. The consolidation induced changes showed positive agreement between the two models (comparing the B orientation of model 31). Both displayed a flattening of curvature in the central part of the figure and the suggestion of an elbow or break.

Model 32. This model was taken from core 68-NB-Station 4, a long Shelby Tube core. The fan-like structure was composed of sandy clay with clay stringers. During consolidation the stringers changed from their uniform curves to more distinctly "S" shaped curves with steep centers and flattened ends. This type of change was also noted in artificial model 6.

Model 33. This model was taken from core 68-NB-Station 4, a long Shelby Tube core. (Immediately above model 32). In this model the structure consisted of bulbous, irregular bodies of sandy clay and clay. The consolidation-induced changes included a bulging of a vertical sandy clay column (33A) and a flattening of the spheroidal shaped sandy clay bodies. These changes closely approximated the type of changes noted in artificial models 2 and 7.

Model 34. This model was taken from core 68-NB-Station 4, a long Shelby Tube core. (Immediately above models 33 and 32). The structure was composed of irregular, random stringers of sandy clay and clay with a spheroidal inclusion of clay (center, lower right quarter of 34A). Adjacent to this inclusion was a gently recurved sandy clay band extending from the bottom center to the upper right of the figure (34A). The post-consolidation radiographs revealed that the consolidation of the clay inclusion allowed the sandy clay band to undergo extreme flattening of its central part, almost to the point of recumbancy. This type of distortion is anticipated by the changes in artificial models 5 and 21. Model 5 suggests the basic change in shape of the central sandy clay band and model 21 indicates the extensive flattening that a clay hemisphere can experience.

Model 35. This model was taken from core 68-NB-SD3, a short Shelby Tube core. The structure consists of vertically oriented asymmetrical arches of silty clay in a dense clay body. A general flattening of curved structures was noted.

COMMENTS AND CONCLUSIONS

The results of this study have given rise to a number of comments and conclusions. The comments are grouped to include the technical developments and general observations.

Comments

General observations

(1) The results obtained during this investigation are based on singular tests. No repetitive tests were conducted on a model type once a successful consolidation was obtained. Therefore, it must be kept in mind that a number of different post-consolidation figures are possible and that the ones used in this study may be atypical. However, the chances of obtaining grossly different end figures seem remote and the figures tested are thought to be sufficient to demonstrate the concept.

(2) The time parameter was tacitly ignored during this research for the following reason. Very little could be done to include a significant time factor in the program. The rate of burial of natural macrostructures ranges in magnitude from a few centimeters per century to a few centimeters per thousand years. Consequently, any practical load application rate would be relatively explosive by comparison.

(3) This program did not involve carbonate sediments. A comprehensive understanding of carbonate chemistry including pressure

phenomena would be necessary before a quanitative program could be started. A considerably more elaborate procedure would probably be necessary.

(4) One method for the analysis of consolidated macrostructures in pelitic sediments would require the following:

(a) Establish a limited catalog of unconsolidated "index" macrostructures from known depositional environments.

(b) Consolidate a number of the index macrostructures.

(c) Develop the artificial geometric models necessary for the interpretation of the consolidated index models.

(d) Test the artificial models developed in (c) under a variety of consolidation conditions and changes of composition.

Using the resulting data, it may be possible to recognize consolidated index macrostructures within a range of variations and relate them to an environment of deposition.

Technical developments

(1) The electro-osmotic knife is an extremely useful device for the undisturbed handling of unconsolidated pelitic sediments. This research project would have been nearly impossible without one. The knife overcomes one of the major hindrances to the study of soft, unconsolidated sediments; the inability to cut them without distortion.

(2) The Flexible Liner concept and the two corers developed around it have proven to be successful in significantly reducing the

amount of damage done to fragile macrostructures in pelitic sediments. Also, the deep water model displayed superior core recovery characteristics in areas where the sedimentary sequence includes very soft clays adjacent to firm layers.

(3) The hydrostatic anchor system used on the shallow water corer may have very broad applications in the field of underwater operations (especially for small submersibles).

(4) Electrical logging of recent sediments is not only a rapid, non-destructive means of locating macrostructures, but also promises to have important applications in a variety of areas of oceanography and ocean engineering.

Conclusions

The following conclusions are based upon the results of the performed research.

(1) Consolidation-induced changes in natural macrostructures of pelitic sediments can be related to changes induced in artificial geometric models under the following conditions:

(a) The composition of the materials making up the natural macrostructures must be duplicated in the geometric models.

(b) The direction of fluid drainage in the natural macrostructure must be known and duplicated in the geometric model processing.

(c) An accurate means of mapping the macrostructures must be available. (Stereo X-ray radiography requires the existence of of X-ray density differences between the materials involved in the structure and the absence of any excessive X-ray density in the matrix material.)

(2) Some quanitative information may be derived from the data gathered from this research. Caution must be exercised to insure the identification and evaluation of all variables that may have influenced the tests.

(3) The experience, methods, and techniques developed during the course of this study could form the basis for designing a quanitative program along similar lines.

REFERENCES

ANBAH, A. S., BEESON, C. M. and CHILINGAR, G. V., 1965. Application of electrokinetic phenomena in civil engineering and petroleum engineering. Ann. New York Academy Sci., 118(14):585-602.

BOUMA, A. H., 1963. A graphic presentation of the facies model of salt marsh deposits. Sedimentology, 2:122-129.

BOUMA, A. H., 1969. Methods for the Study of Sedimentary Structures. John Wiley & Sons, N. Y., 458 pp.

BOUMA, A. H. and BOERMA, J. A. K., 1968. Vertical disturbances in piston cores. Marine Geol., 6:231-241.

BOUMA, A. H. and MARSHALL, N. F., 1964. A method for obtaining and analyzing undisturbed oceanic sediment samples. Marine Geol., 2:81-99.

BOUMA, A. H., REZAK, R. and CHMELIK, F. B., 1969. Sediment transport along oceanic density interfaces. (abstract only) A.A.P.G. Ann. Meeting, Atlantic City, N. J., 1969, pp. 259-260.

BOWLES, F. A., 1968. Electron microscopy investigation of the micro-structure in sediment samples from the Gulf of Mexico. Tech. Rept. 68-24T, Dept. Ocean., Texas A&M University, 132 pp.

BOYCE, R. E., 1967. Electrical Resistivity of Modern Marine Sediments from Bering Sea. M.S. Thesis, San Diego State College, San Diego, Calif., 172 pp.

BRIGGS, L. I. and MIDDELTON, G. V., 1965. Hydromechanical principles of sediment structure formation. Soc. Econ. Paleon. and Miner., Spl. Pub., 12:5-16.

BROWN, G. H., 1967. Liquid crystals. Chemistry, 40:10-18.

BROWN, G. H., DIENES, G. J. and LABES, M. N., 1965. Liquid Crystals. Gordon and Breach Sci. Pub., N. Y., 35 pp.

BROWN, G. H. and SHAW, W. G., 1957. The mesomorphis state, liquid crystals. Chemical Reviews, 57:1049.

BRUSH, L. M., 1965. Experimental work on primary sedimentary structures. Soc. Econ. Paleon. and Miner., Spl. Pub., 12:17-24.

BRYANT, W. R., CERNOCK, P. J. and MORELOCK, J., 1967. Shear strength and consolidation characteristics of marine sediments from the western Gulf of Mexico. In: A. Richards, (Editor) Marine Geo-technique, University of Illinois Press, Urbana, Ill., pp. 41-49.

BUCHANAN, P. N., 1964. Effects of Temperature and Adsorbed Water on Permeability and Consolidation Characteristics of Sodium and Calcium Montmorillonite. Ph.D. Dissertation, Texas A&M University, 119 pp.

CASAGRANDE, I. L., 1941. The drainage of fine soils. Strasse, 8(19/20):324.

CAYEUX, L., 1941. Causes Anciennes et Causes Actuelles in Geologie. Masson, Paris, 81 pp.

CERNOCK, P. J., 1967. Consolidation Characteristics and Related Physical Properties of Selected Sediments from the Gulf of Mexico. M.S. Thesis, Texas A&M University, 137 pp.

CHMELIK, F. B., 1967. Electro-osmotic core cutting. Marine Geo., 5:321-325.

CHMELIK, F. B., 1968. Sediment probes and anchor system for submersible research vehicles. Trans. Marine Tech. Soc., Washington, D. C., pp. 503-526.

CHMELIK, F. B., 1969. Thermal properties of marine sediments. Trans. Marine Temp. Measur. Sym., Marine Tech. Soc., Washington, D. C., pp. 275-288.

CHMELIK, F. B., (in preparation) A shallow water corer.

CHMELIK, F. B., BOUMA, A. H. and BRYANT, W. R., 1968. Influence of sampling on geologic interpretations. Trans. Gulf Coast Assoc. Geol. Soc., Jackson, Mississippi, 28:256-263.

CHMELIK, F. B. and BOUMA, A. H., 1969a. Electrical logging of recent marine sediment cores. In: A. H. Bouma, W. R. Bryant and D. K. Davies, Topics and Techniques, Gulf of Mexico, Texas A&M University, Dept. Ocean., U. S. Geological Survey Contract. No. 14-08-0001-10866 Ref. 69-5T Proj. 506, pp. 107-116.

CHMELIK, F. B. and BOUMA, A. H., 1969b. Electrical logging of recent marine sediments. (abstract only) Trans. Amer. Geoph. Union., Washington, D. C., 50(4):201.

CHMELIK, F. B. and BOUMA, A. H., 1969c. Electrical logging in recent sediments. (in print) Trans. 2nd Amer. Offshore Tech. Conf., Houston, Texas, June 1970.

CHMELIK, F. B., BOUMA, A. H. and REZAK, R., 1969d. Comparison of electrical logs and physical parameters of marine sediment cores. Trans. 19th Ann. Meeting, Gulf Coast Assoc. Geol.Soc., Miami, Fla. pp. 63-70.

CHUBER, S. and PUSEY, W. C., 1967. Cyclic San Andres facies and their relationship to diagenesis, porosity and permeability in the Reeves Field, Yoakum County, Texas. In: Cyclic Sedimentation of the Permian Basin, Texas, Western Geological Society, Midland, Texas. pp. 136-151.

COLEMAN, J. M. and GAGLIANO, S. M., 1965. Sedimentary structures: Mississippi River deltaic plain. Soc. Econ. Paleon. and Miner., Spl. Pub., 12:133-148.

COOGAR, A. H., 1967. Recent and ancient carbonate cyclic sequences. In: Cyclic Sedimentation of the Permian Basin, Texas, Western Geological Society, Midland, Texas, pp. 5-16.

EWING, M., 1955. The ice-age theory. J. Alberta Soc. Petrol. Geol., 8:191-201.

GREENSMITH, J. T., 1966. Carboniferous deltaic sedimentation in Eastern Scotland: a review and reappraisal. In: Deltas in Their Geologic Framework, Houston Geological Society, Houston, Texas, pp. 89-211.

HAASE, M. C., 1967. X-ray radiographs of unopened cores. Misc. Paper N. 3-918, U. S. Army Corps of Engr. Waterways Experimental Station, Vicksburg, Mississippi., 40 pp.

HAMBLIN, W. K., 1962. X-ray radiography in the study of structures in homogeneous sediments. J. Sediment. Petrol., 32:201-210.

HAMILTON, E. L., 1959. Thickness and consolidation of deep-sea sediments. Bull. Geol. Soc. Amer., 70:1399-1424.

HOROWITZ, D. H., 1967. Evidence for deltaic origin of an Upper Oroevician sequence in the Central Appalachians. In: Deltas in Their Geologic Framework, Houston Geological Society, Houston, Texas, pp. 160-169.

HUTT, J. R. and BERG, J. W., 1966. Thermal and electrical conductivities of ocean sediments and sandstone rocks. Dept. Ocean., Oregon State University, Corvalles, Oregon. (submitted to Geophysics, Dept. 1966).

HVORSLEV, M. J., 1940. Soil Mechanics and Its Application. Purdue University Press, Lafayette, Ind., 87 pp.

HVORSLEV, M. J. and STETSON, H. C., 1946. Free-fall coring tube: a new gravity bottom sampler, Bull. Geol. Soc. Amer., 57:935-950.

JACKA, A. D., THOMAS, C. M., BECK, R. H., WILLIAMS, K. W. and HARRISON, S. C., 1967. Guadalupian depositional cycles of the Delaware Basin and Northwest Shelf. In: Cyclic Sedimentation of the Permian Basin, Texas, Western Geological Society, Midland, Texas, pp. 152-196.

KERMABON, A., CEHIN, C. and BLAVIER, P., 1965. Relationship between porosity, density, and electrical resistivity of some unconsolidated deep sea sediments taken from the Tyrrhenean Sea. (pre-report) Sarlant ASW Center, La Spezia, Italy, 22 pp.

KOLB, C. R. and VAN LOPIK, J. R., 1966. Depositional environments of the Mississippi River deltaic plain, Southwestern Louisiana. In: Deltas in Their Geologic Framework, Houston Geological Society, Houston, Texas, pp. 17-61.

KRINITZSKY, E. L. and SMITH, F. L., 1969. Geology of backswamp deposits in the Atchafalaya Basin, Louisiana. Tech. Rept. S-69-8, U. S. Army Corps of Engr. Waterways Experimental Station, Vicksburg, Mississippi, 70 pp.

KRUMBINE, W. C. and SLOSS, L. L., 1951. Stratigraphy and Sedimentation. W. H. Freeman & Co., San Francisco,Calif., 660 pp.

KRUYT, H. R., 1952. Colloid Science. Elsevier Publ Co., N. Y., 1: 389 pp.

KULLENBURG, B., 1947. Deep-sea coring. Reports of the Swedish deep-sea expedition, IV, Bottom investigations, 2. pp. 37-96.

LOWE, J., ZACCHEO, P. R. and FELDMAN, H. S., 1964. Consolidation testing with back pressure. J. Soil Mechanics and Foundations Division, Amer. Soc. Civil Engr., 90:69-86.

MONROE, J. N., 1969. Slumping structures caused by organically derived gasses in sediments. Science, 164(3886):1394-1395.

MOORE, D. G. and SCRUTON, P. C., 1957. Minor internal structures of some recent unconsolidated sediments. Bull. Amer. Assoc. Petrol. Geol., 41:2723-2751.

PAUTOT, G., 1967. Measures de resistivities sur des carottes de sediments marine et lacustres. Bull. Inst. Ocean. Monaco., 67:1376-1383.

PETTIJOHN, F. J., 1949. Sedimentary Rocks. Harper & Brothers, N. Y., 526 pp.

PIRSON, S. J., 1963. Handbook of Well Log Analysis. Prentice-Hall, Englewood Cliffs, N. J., 326 pp.

QUINCKE, G., 1861. Pogg. Ann. Physik., 113:513; quoted in Smoluchowski. Smoluchowski, Von M., 1921. Electric endosmosis and streaming current. In: Handbuch der Elecktrizitat und des Magnetisusm. 2:366-428. Trans. by P. E. Bocque, University Mich. Engr. Res. Bull., 33:47-158.

RAINWATER, E. H., 1966. The geologic importance of deltas. In: Deltas in Their Geologic Framework, Houston Geological Society, Houston, Texas, pp. 1-15.

REINECK, H. E., 1967. Layered sediments of tidal flats, braches, and shelf bottoms of the Borth Sea. In: Estuaries, Pub. No. 83, Amer. Assoc. for the Adv. of Sci., Washington, D. C., pp. 191-206.

SANDERS, J. E., 1965. Primary sedimentary structures formed by turbidity currents and related resedimentation mechanisms. Soc. Econ. Paleon. and Miner., Spl. Pub. 12, pp. 192-219.

SHEPARD, F. P., 1964. Criteria in modern sediments useful in recognizing ancient sedimentary environments. In: L. M. J. U. van Straaten, (Editor) Deltaic and Shallow Marine Deposits, Elsevier Pub. Co., N. Y., 464 pp.

SMITH, H. T. U., 1943. Aerial Photographs and Their Applications. Appleton-Century-Crofts, N. Y., 372 pp.

STANLEY, D. J., 1966. Petrology and stratigraphy applied to a problem of river engineering in the lower Mississippi delta. In: Deltas in Their Geologic Framework, Houston Geological Society, Houston, Texas, pp. 63-81.

TAYLOR, D. W., 1948. Fundamentals of Soil Mechanics. John Wiley & Sons, N. Y., 700 pp.

TERZAGHI, K., 1955. Influence of geological factors on the engineering properties of sediments. Econ, Geol., 15:557-618.

VAN STRAATEN, L. M. J. U., 1961. Sedimentation in tidal flat areas.

J. Alberta Soc. Petrol. Geol., 9:203-226.

WU, T. H., 1967. Soil Mechanics. Allyn & Bacon, Inc., Boston, Mass., 431 pp.

APPENDIX I

Stereo X-ray radiography

Introduction

The application of X-ray radiography to the study of sediments dates back only to 1962 (Hamblin). The concept is basically similar to industrial radiography. A sedimentary sample is placed on a piece of photo-sensitive film. X-radiation is allowed to pass through the sample and onto the film. The film is exposed differentially in response to:

(1) power characteristics of the X-ray source,

(2) distance from the radiation source to the sample (and film),

(3) total thickness of the sample,

(4) sensitivity of the film to the radiation,

(5) density differences within the sample, and

(6) mineralogy of the sample.

The last two items are the independent variables of interest in the study of sedimentary macrostructures. BOUMA (1969) presents an excellent review not only of previous work in this field but also of the important contributions made by him on methodology and interpretation.

Discussion

The use of stereo radiography opens a new avenue of approach to the study of sedimentary macrostructures. Two important qualities are inherent in stereo radiography; first, it is a non-destructive technique and second, three dimensional spatial relationships can be realized within the sample. This combination is unique to stereo radiography. The stereo radiological method used in this study consists of making one exposure with the sample located to the left of center of the field of radiation and another with the sample to the right of center. The horizontal displacement across the center point was 3.15 in. (8 cm.). During each exposure, the portion of the film not to be exposed was protected by a lead shield. (Fig. AI-1). The stereo effect was created by moving the sample between exposures, while allowing the X-ray source to remain stationary. The horizontal axis of displacement passed through the center of the sample. This avoided problems involving parallax along the long axis of the sample cylinders. It was more convenient to move the relatively small-sized samples than to relocate the energy source. Knowledge of the exposure geometry (focal distance, 27 in.; stereo base, 3.15 in.; target, 0.0187 in.) makes it theoretically possible to quantitize spatial relationships within the sample by applying basic photogrammetric techniques (SMITH, 1943).

To insure complete coverage of the figure within a model, stereo radiography was carried out for several model orientations. These included A @ 0^o, B @ 90^o, C @ 45^o, and D @ $22\frac{1}{2}^o$. A was established along a plane of symmetry in the artificial models and at random in the natural ones. The angles indicate the number of degrees the model cylinder was rotated with respect to A and the vertical.

technique and second, three dimensional spatial relationships can be realized within the sample. This combination is unique to stereo radiography. The stereo radiological method used in this study consists of making one exposure with the sample located to the left of center of the field of radiation and another with the sample to the right of center. The horizontal displacement across the center point was 3.15 in. (8 cm.). During each exposure, the portion of the film not to be exposed was protected by a lead shield. (Fig. AI-1). The stereo effect was created by moving the sample between exposures, while allowing the X-ray source to remain stationary. The horizontal axis of displacement passed through the center of the sample. This avoided problems involving parallax along the long axis of the sample cylinders. It was more convenient to move the relatively small-sized samples than to relocate the energy source. Knowledge of the exposure geometry (focal distance, 27 in.; stereo base, 3.15 in.; target, 0.0187 in.) makes it theoretically possible to quantitize spatial relationships within the sample by applying basic photogrammetric techniques (SMITH, 1943).

To insure complete coverage of the figure within a model, stereo radiography was carried out for several model orientations. These included A @ 0^{o}, B @ 90^{o}, C @ 45^{o}, and D @ $22\frac{1}{2}^{o}$. A was established along a plane of symmetry in the artificial models and at random in the natural ones. The angles indicate the number of degrees the model cylinder was rotated with respect to A and the vertical.

Fig. AI-1. Physical arrangement for stereo X-ray radiography. Individual models are shot first at one side of center then at the other. Model cylinders are ballasted in quartz sand to reduce exposure variations. Several model orientations are used to insure complete coverage. The two sample exposure method reduces processing time.

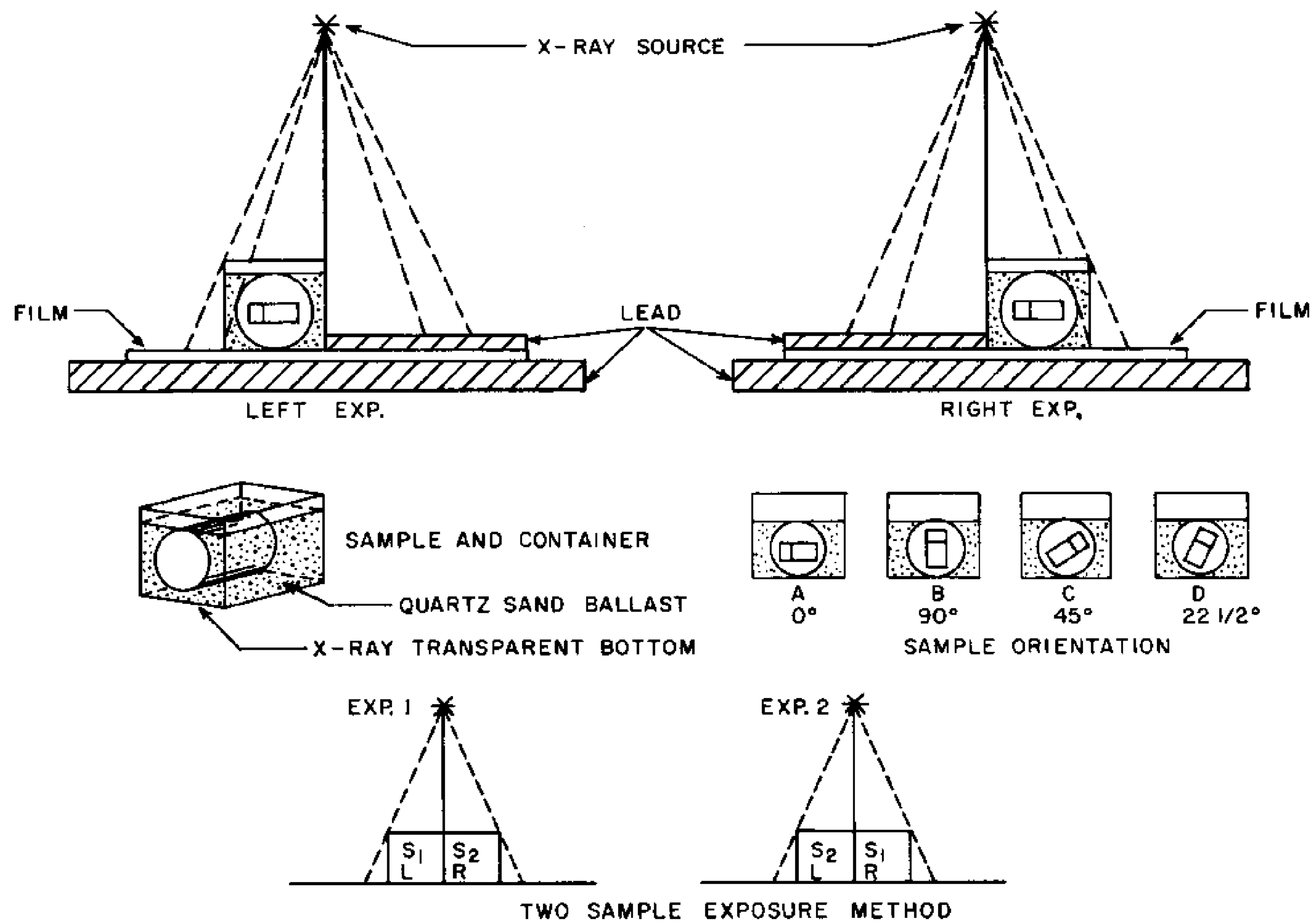
X-RAY SOURCE
FILM
LEAD
FILM
LEFT EXP.
RIGHT EXP.
SAMPLE AND CONTAINER
QUARTZ SAND BALLAST
X-RAY TRANSPARENT BOTTOM
A
0°
B
90°
C
45°
D
22 1/2°
SAMPLE ORIENTATION
EXP. 1
S1 L
S2 R
EXP. 2
S2 L
S1 R
TWO SAMPLE EXPOSURE METHOD

The models were cylindrical and required ballasting to insure optimum exposure. (Exposure variation occurs due to the difference in thickness of material penetrated by the X-rays at the edge of a cylinder as opposed to the center.) Clean, well-sorted, fine-grained quartz sand was used for ballast. Cardboard boxes with plexiglass bottoms (X-ray transparent) were used to hold the sample cylinders and ballast during exposure. The sand, filling the box to the top of the cylinder, helped maintain the cylinder in the desired orientation and brought the X-ray density across the entire sample to an acceptable level (the sand creates a negligible pattern on the radiographs). To reduce the time required for radiography, a two sample exposure system was used. This simply consists of exposing the right stereo shot of one model simultaneously with the left stereo shot of another.

APPENDIX II

Sample preparation by electro-osmosis

Introduction

Preparation of both natural and artificial macrostructure models required a technique producing little or no mechanical distortion. No such technique was available.

By the application of the principle of electro-osmosis, it was possible to cut soft pelitic materials into required shapes without distorting the incorporated macrostructures. The time required for sample preparation was significantly reduced. Freedom from distortion of the structures facilitated testing and the interpretation of the results.

Discussion

The electro-osmotic effect in clay is by no means new. QUINCKE (1861, in KRUYT, 1952) was probably the first scientist to predict a technical application of electro-kinetics. Several patents on the removal of water from clay by electro-osmosis were issued in Germany before World War II (CASAGRANDE, 1941, ANBAH, 1965). The theoretical aspect of electro-osmosis involves: (1) a net negative electrical charge on the clay particles, (2) the existence of an electrical double layer, (3) small diameter interconnecting pores which act as capillary tubes throughout the clay mass, and (4) a d-c electrical potential applied across the clay mass. The d-c potential forces the interstitial fluid to migrate through the clay from the positive electrode to the negative electrode. This migration was used to continuously lubricate the contact surface of cutting and shaping devices during preparation of the clay samples. The electro-osmotic effect was applied to a sediment knife, several specially shaped cutting devices used in fabricating the geometric models and to the ring used for cutting the samples for consolidation. (Fig. AII-1). It was found that a maximum of 50 vdc at 4 amps, was sufficient for virtually all laboratory work (CHMELIK, 1967; BOUMA, 1969). BOWLES (1968), in preparing small clay samples for electron microscopy, used a 1.5v dry cell and segments of a stainless steel razor blade.

A note of caution. When using high power settings, this equipment will unpleasantly reprimand the operator who inadvertently becomes part of the circuit. The isolation transformer and power relay do much to prevent accidental shock, but do nothing to insure against operator inattention.

Fig. (AII-I). Electro-osmotic sample cutting device. The device consists of an isolated, variable power d-c power supply with a selection of cutting and shaping tools. All tools act as negative electrodes.

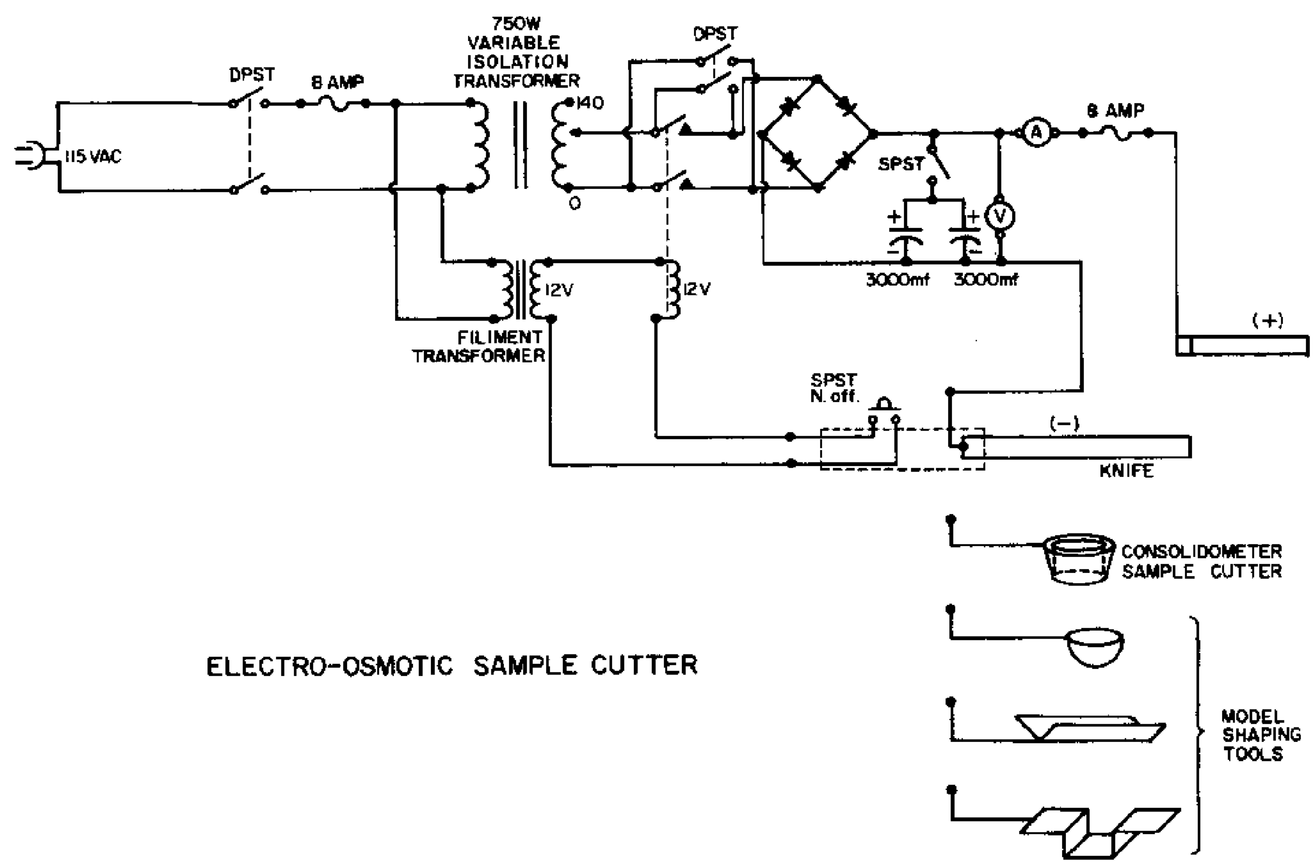

ELECTRO-OSMOTIC SAMPLE CUTTER

APPENDIX III

Sampling techniques - Flexible Liner corers

Introduction

Macrostructures in recently accumulated sediments are usually very fragile and subject to distortion by sampling devices. Technically, there is no such thing as an "undisturbed" sample. The act of taking a sample (i.e., removing an amount of material from its natural surroundings) always introduces some disturbance. A limit of tolerable disturbance is set by the nature of the investigation involved. In the case of recent macrostructure studies, this limit approaches zero.

Discussion

HVORSLEV (1940) listed five basic types of disturbance caused by sampling devices:

(1) changes in stress conditions

(2) changes in water content

(3) disturbance of sedimentary structures

(4) changes in thickness of sedimentary layers

(5) mixing of sedimentary layers.

He also states that the primary cause of sample disturbance is the frictional drag between the sample and the inside wall of the core barrel (HVORSLEV, 1940, HVORSLEV and STETSON, 1946). Many attempts have been made to solve this problem. Piston corers, with and without liners, help to some degree (KULLENBURG, 1947; EWING, 1955).

However, it is estimated that samples may be shortened by as much as 50% in these devices. Shortening probably takes place when a soft layer is squeezed out from between two firmer layers. This concept has been tentatively confirmed by this author (CHMELIK,et al., 1968).

Flexible Liner Corer

In order to preserve fragile macrostructures in core samples, the problem of disturbance was approached from a different viewpoint. A free-fall, piston corer was designed and built utilizing a flexible liner to minimize the effect of wall friction (Fig. AIII-1). Stored in the coring head, the flexible liner completely encases the sample as it enters the device and prevents it from coming in contact with the inside wall of the barrel (Fig. AIII-2).In addition, the liner retards fluid loss by its relative impermeability, tends to keep the sediment layers in place by adhesion and cohesion, and makes it possible to treat the core and liner as a single unit. Theoretically, the "barrel" could consist of a simple arrangement of rods whose only function would be to push the corehead into the sediments.

Fig. AIII-1. Flexible Liner Corer.
1. Core barrel
2. Piston assembly
3. Outer casing
4. Flexible Liner
5. Liner supply cylinder
6. Core catcher
7. Cutting head

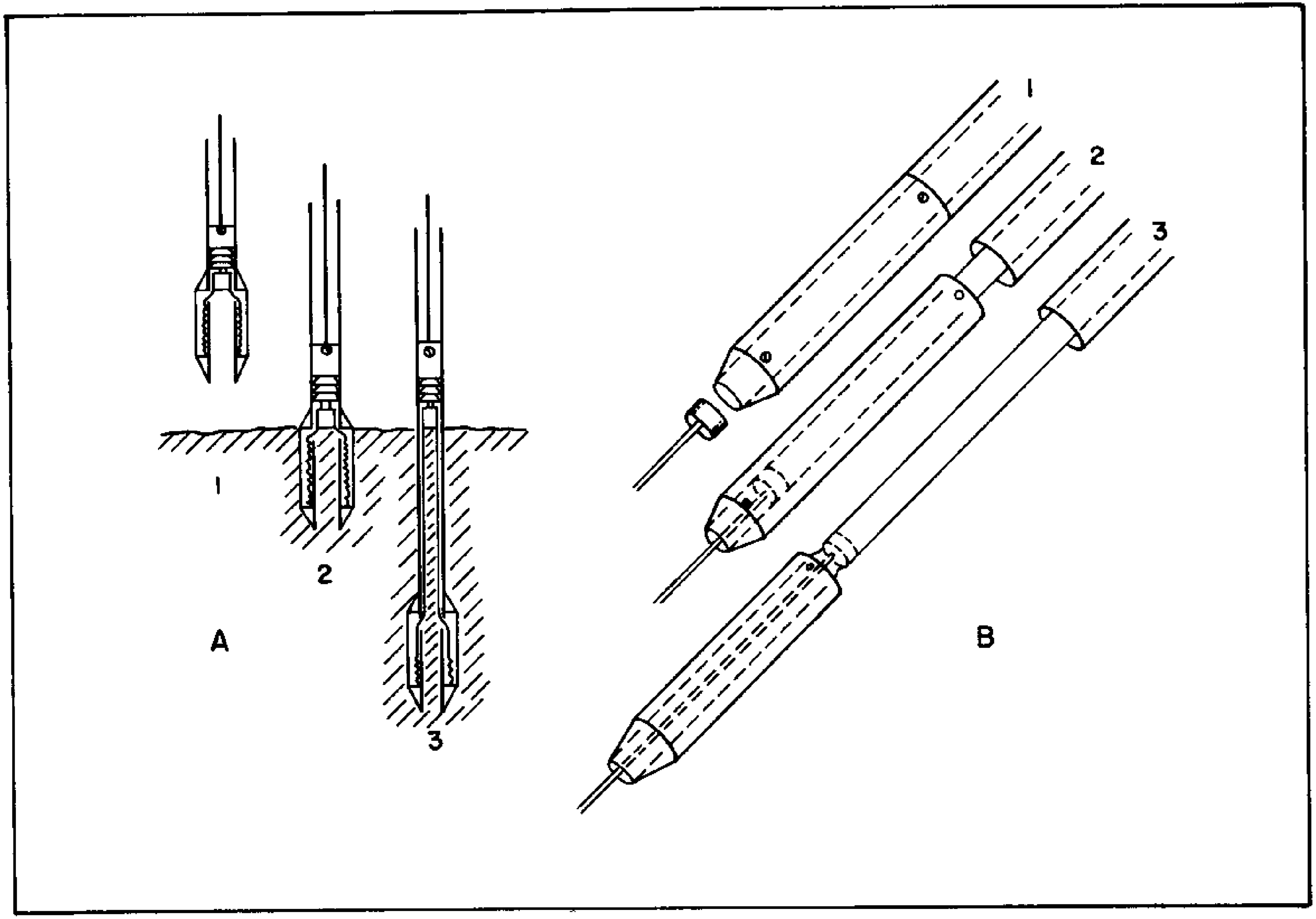
1
2
3
A
1
2
3
B

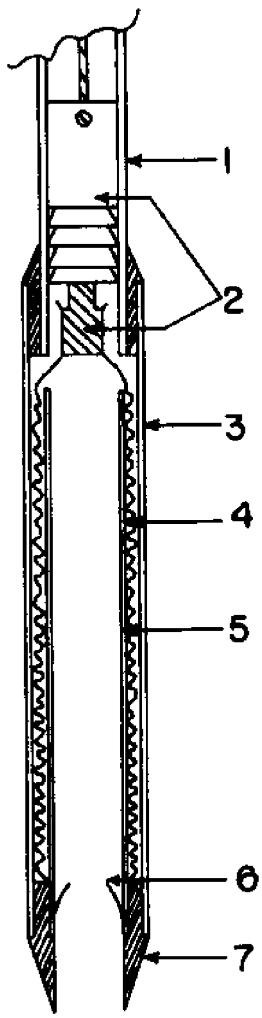

1
2
3
4
5
6
7

Fig. AIII-2. Deep Water Flexible Liner corer.

A. Operation of Flexible Liner corer
   1. lowering configuration
   2. start of coring
   3. corer penetrating sediments

B. Post-coring removal of core head
   1. extrusion block in place
   2. core head detached from barrel and moving over extrusion rod
   3. extrusion complete - block at end of rod is sealed into end of liner

The writer designed and constructed this flexible liner corer at Texas A&M University in the Spring of 1965. Later, similar devices were developed independently by other investigators. This sequence of events was confirmed by DR. A. M. ROSFELDER of Scripps Institution of Oceanography (personal communication, March, 1967).

The first model of the Flexible Liner corer was suitable for use in all depths of water. (CHMELIK,et al., 1968). A second model was designed and built specifically for use in the shallow water (diver depth or less) of bays and estuaries.

Shallow Water Corer

Soft sediments found in bays and estuary-type environments (shallow water; low, swampy margins) are difficult to core. The problem is basically one of physical conditions of the local introducing practical limits on the size and complexity of the equipment. These areas are usually too shallow for ships and too wet for land vehicles.

Shelby tubes have been successfully used but are limited in length and diameter by the units of "effective man-effort" available for coring operations. (One unit of effective man-effort is defined here as the capability of a man to perform similar operations unencumbered by mud and/or water. This is a qualitative term used for rough comparisons only.)

A shallow water corer was built to facilitate sampling in these different areas (CHMELIK, in preparation). It was designed to meet the following requirements:

(1) independent of shipboard power

(2) light enough to be handled by two men (in units of effective man-effort)

(3) capable of using the ground as reference

(4) take a core with the lowest disturbance tolerance possible

(5) provide a mechanical means of operation using not more than one-half unit of effective man-effort, and

(6) include a way of protecting the core while being transported from the site.

The design requirements describe a light weight Flexible Liner corer with a mechanical drive and an anchor system to hold it firmly to the bottom. The problems of weight and mechanical drive were solved by using an open frame of light angle iron and two hand-cranked winches (Figs. AIII- 3,4). Since the original unit was built for use on a floating platform raft, it was convenient to mount the winches on a light davit used to swing the corer over the side. Three hydrostatic anchors were used to hold the corer firmly to the bottom (CHMELIK, 1968). These were set by opening the valves, standing on them until they were implanted in the bottom, and then closing the valves. Release was effected by opening the valves and pulling upward on the entire unit. No difficulty was experienced in either operation. A small, electrically driven centrifugal pump was successfully used to manipulate the hydrostatic anchors, but was found to be less convenient than the manual method. This pump was connected to the anchors via a system of hoses and valves. (Fig. AIII-5). With the anchors resting on the bottom, the pump moved water out of the anchors and the hydrostatic pressure forced them into the sediments. With the valves closed, each anchor had a holding force of approximately 1,000 pounds. Release of the anchors was accomplished by reversing the pump and forcing water into the anchors.

Once the corer was recovered, the cutting head, top fitting, and piston were removed from the core barrel. (Fig. AIII-6). The barrel, with the liner and core suspended inside, was then sealed at the bottom and filled with local water to prevent dehydration and lessen shock. The top was sealed and the barrel used as a container for the protection of the core during transporting. The core barrels were 4½ ft. sections of 4 in. diameter downspout pipe. The flexible liners were 3.5 in. in diameter. This arrangement facilitated taking a four-foot long, 3.5 in. diameter sample.

Fig. AIII-3. Shallow water Flexible Liner corer with hydrostatic anchors.

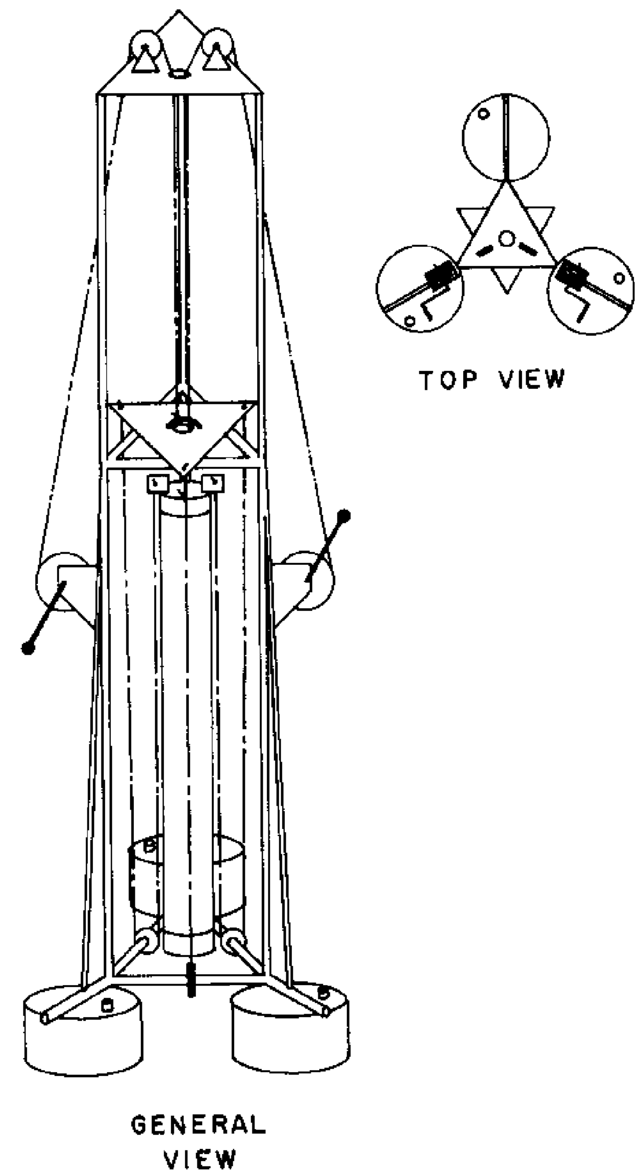
TOP VIEW
GENERAL
VIEW

Fig. AIII-4. Operation of shallow water corer.
A. Corer on bottom (anchors set)
B. Core barrel winched into sediments
C. Core barrel and sediments winched free of bottom

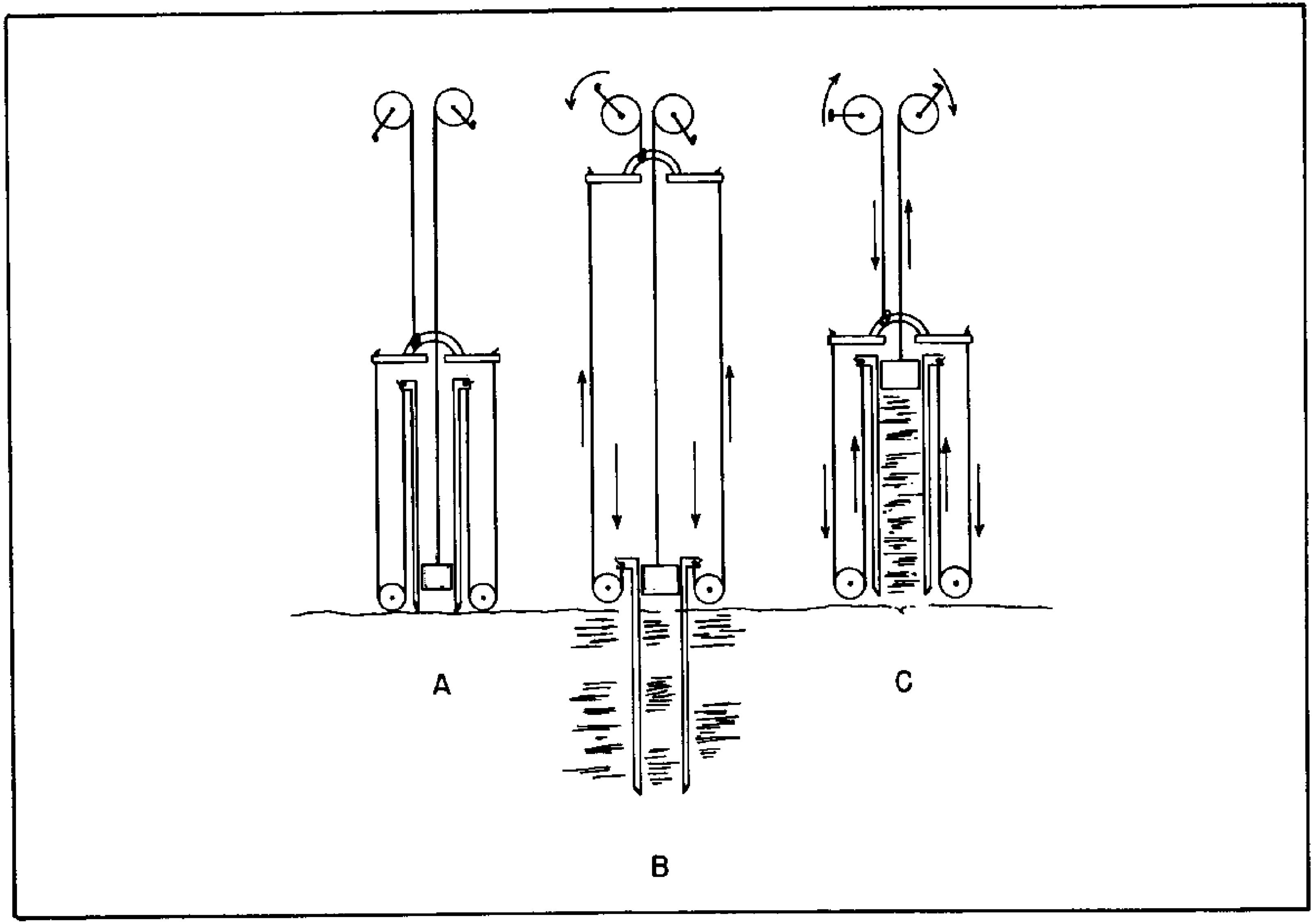
A
B
C

Fig. AIII-5. Hydrostatic anchor principle.
A. Anchors on bottom at the start of water pump-out. Hydrostatic pressure on top of anchors forces them into the sediments.
B. Anchors locked on bottom.
C. Release from bottom effected by pumping water into anchors.

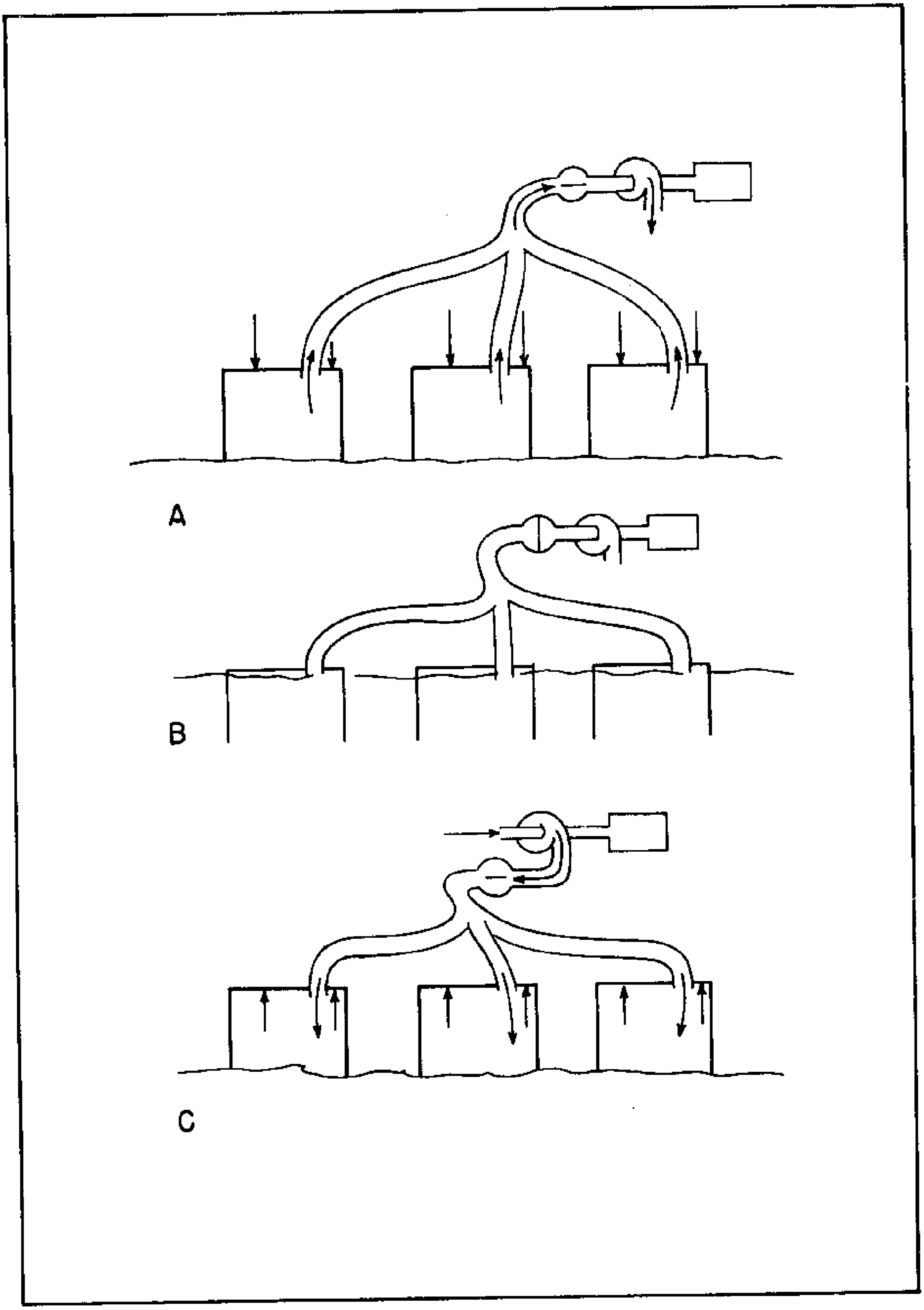
A
B
C

Fig. AIII-6. Shallow water corer.

A. Piston assembly
   1. Bail
   2. Ball valve
   3. Metal flange
   4. Rubber gasket
   5. Plywood coated with epoxy
   6. Retaining bolt for wood piston
   7. Air channel
   8. Hole for hanger rod
   9. Wood piston (plywood)

B. Core barrel assembly
   1.,2. Top mount with winch cable attachment holes
   3. Four inch dia., 4½ ft. long core barrel
   4. Flexible liner
   5. Liner supply cylinder
   6. Handling legs
   7. Cutting head
   8. Core catcher

C. Sample prepared for transport and storage
   1. Sheet plastic cover
   2. Hanger rod
   3. Water ballast
   4. Wood piston
   5. Sample
   6. Core barrel
   7. Bottom plug
   8. Plastic cap sealing bottom of core barrel

Flexible liner is tied-off at wood piston (No. 4) and bottom plug (No. 7).

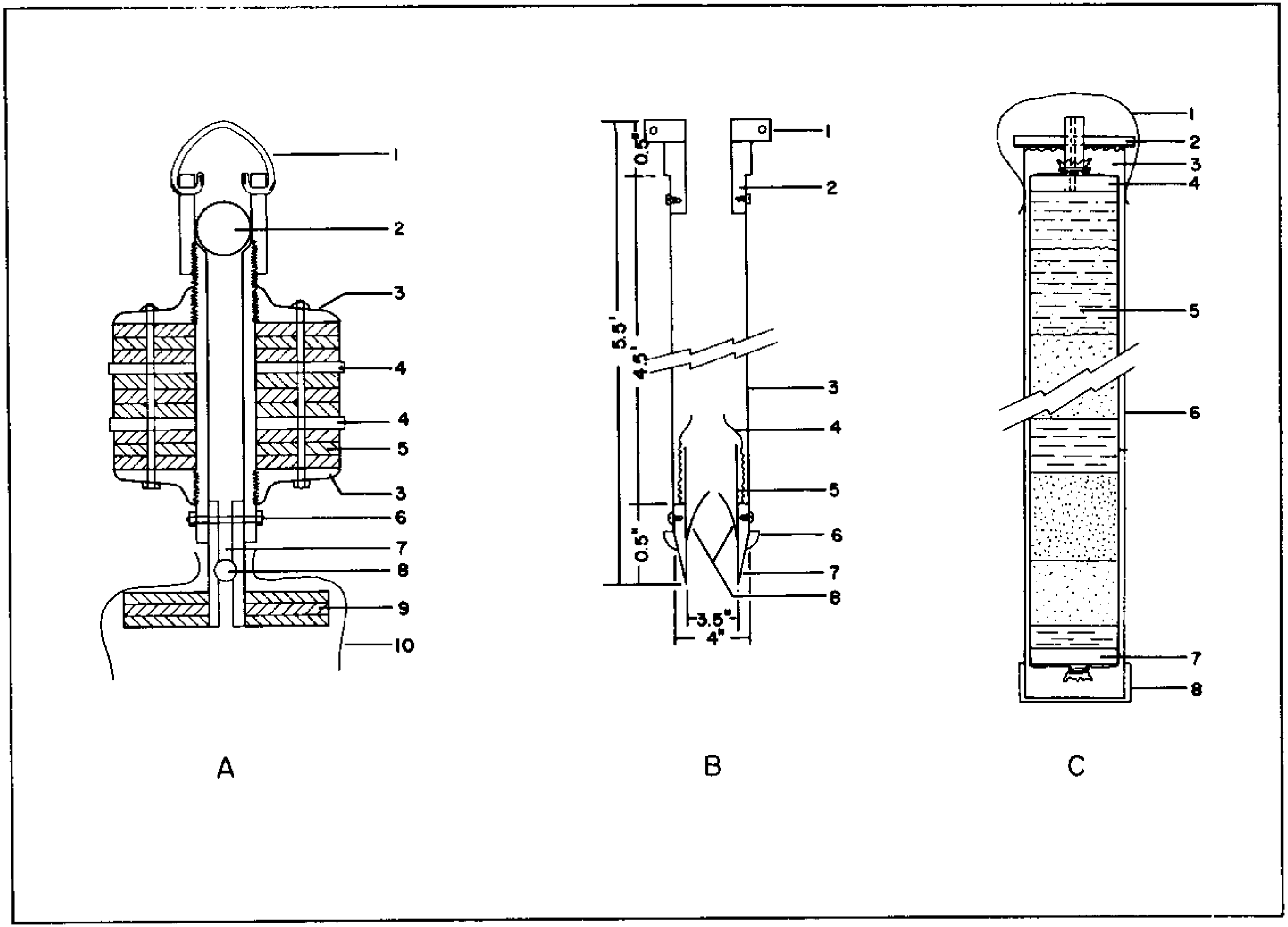
1
2
3
4
4
5
3
6
7
8
9
10
A
0.5"
5.5'
4.5'
0.5"
3.5"
4"
1
2
3
4
5
6
7
8
B
1
2
3
4
5
6
7
8
C

APPENDIX IV

Electrical logging

Introduction

Electrical logging (PIRSON, 1963) a geophysical technology highly developed by the petroleum industry, has remained a relatively untapped source of methodology for the study of recent sediments.

A few exceptions are found in the literature. KERMABON, GEHIN, and BLAVIER (1965) relate porosity, density and electrical resistivity. HUTT and BERG (1966) presents a relationship between electrical and thermal conductivity. PAUTOT (1965) described a method for using electrical resistivity logging for correlating between cores taken from the same lacustrine area. BOYCE (1967) made a number of absolute measurements of electrical resistivity in recent marine sediment cores. Of these investigators, only KERMABON, GEHIN, and BLAVIER used a technique that resulted in a set of continuous curves and *in situ* measurements.

Continuous point resistivity and spontaneous potential logging techniques have been developed at Texas A&M which allow both *in situ* and laboratory measurements of the electrical properties of recent sediments. (CHMELIK, et al., 1969 a, b, c, d; BOUMA, et al., 1969) The initial results of this work indicates that quantitative relationships exist between the electrical properties and other physical and chemical properties of sediments. Correlation between core stations and between a core and the logs taken at the same station afford a means of tracing horizons and evaluating the quality of cores.

Electrical logs are useful as a non-destructive means of identifying sedimentary zones of interest in cores and *in situ*. These zones of interest are intervals where changes in the sediments occur and are often too subtile to easily detect by other means. Among these zones are intervals along the core where sedimentary macro-structures are concentrated. These concentrations show up on the electrical logs as places where the curves are very complex indicating rapid changes in the electrical characteristics. Logging thus makes available a means of rapidly locating probable macrostructure zones in a core thus reducing the necessity of taking radiographs of the entire core for such studies.

APPENDIX V

Color thermography

Introduction

Investigations on thermal properties of sediments have been hindered by (a) lack of resolution, (b) lack of definition, and (c) thermal interference due to instrumentation. The application of cholesteric liquid crystals to the study of sediment thermal properties offers a partial solution to the problem.

Discussion

When illuminated with white light, cholesteric liquid crystal structures scatter the light to a given irridescent color which varies with the character of the substance, the temperature and the angle of incidence. The liquid crystals change color through the visible spectrum in response to changes in temperature; each color characteristic for a given set of conditions (BROWN and SHAW, 1957).

The color scattered by any one liquid crystal compound is unique for a specific temperature (assuming constant lighting, etc.) and thus allows for the quantitative measurement of temperature. Spectral shift per unit change in temperature is nearly linear (BROWN, DIENES and LABES, 1966). Resolution of 20 line pairs per millimeter and a response time of less than one second may be expected (BROWN, 1967).

Laboratory evaluation of liquid crystal technology as applied to the study of macrostructures in recent sediments indicated that water content and lithology effected the thermal properties to a greater extent than anticipated (CHMELIK, 1969). In saturated, porous sediments the water apparently acts as a thermal diffusing agent and hinders the development of sharp thermal boundaries. The exercise supports the findings of HUTT and BERG (1966) who related thermal and electrical conductivities in recent marine sediments. This relationship is based on the water content and lithology of the material.

The initial investigation involved sixteen macrostructure models, both natural and artificial. The results indicated that the technique would require elaborate laboratory equipment and complex sample preparation procedures before being applicable to this dissertation research problem. Consequently, it was decided to temporarily abandon this line of investigation.